The heteroclinic and codimension-4 bifurcations of a triple SD oscillator

Xinyi Huang · Qingjie Cao

Abstract In this paper, the complicated heteroclinic and codimension-four bifurcations of a triple SD (smooth and discontinuous) oscillator are investigated by analyzing the bifurcation sets in three-dimensional parameter space. The structure of the transition set including the equilibrium bifurcation set and a special kind of heteroclinic orbit bifurcation set is constructed comprising of a catastrophe point of the fifth order, the catastrophe curves of third order and also the catastrophe surfaces of the first order, respectively, according to the restoring forces and also the potentials, respectively. Also, a theorem of structural stability of heteroclinic orbit in 2-dimensional Hamilton system is introduced to find the heteroclinic bifurcation set. The equilibria and the phase structures are classified and shown in details on the transition set and the enclosed structurally stable areas for smooth and discontinuous cases, respectively. The normal forms for each bifurcation surface are built up showing the complex supercritical subcritical pitchfork bifurcations and also the double saddle-node bifurcations, along with the bifurcations of homoclinic and heteroclinic orbit. Taken one of the bifurcation surfaces as an example, the complicated bifurcation is investigated by employing subharmonic Melnikov functions including Hopf, double Hopf, the closed orbit and also the homoclinic/heteroclinic bifurcations. The results presented herein this paper enriched the complex dynamic behavior for the geometrical nonlinear systems.

1 Introduction

Nonlinear oscillators [1] play an important role in both science and technology, and they have been widely applied in engineering [2–4], vibration control [5–10], biology [11–13] and electronics [14–16]. Some classical oscillators have been studied for over a century, such as Duffing oscillator [17] proposed in 1918, which is a traditional model to describe the hardening spring effect observed in many solid mechanical problems. Many nonlinear systems can be approximately studied with Duffing system after Taylor expansion, which is of great help in both science and engineering [18,19]. Also, van der Pol Oscillator [20] is a classical oscillator with nonlinear damping exhibiting a limit cycle [21], which has been studied for over a long time. Chaos is first noticed by Ueda [22] in his research on Duffing oscillator with harmonic force, and a chaotic attractor is also found in a set of ordinary differential equations for fluid convection by Lorenz [23].

X. Huang · Q. Cao (✉)
School of Astronautics, Harbin Institute of Technology, Harbin, China
e-mail: qingjiecao@hotmail.com

X. Huang
e-mail: 22b918007@stu.hit.edu.cn

An archetype smooth and discontinuous oscillator comprising lumped mass and oblique springs was proposed by Cao et al. [24] in 2006 to study transition from smooth to discontinuous dynamics. This oscillator has attracted many investigations, demonstrating Hopf bifurcation under nonlinear damping [25], co-dimension two bifurcation [26], chaotic threshold [27], the transition of resonance mechanisms [28] and so on [29]. Later, the coupled SD oscillator was proposed by Han et al. [30] with two geometrical parameters exhibiting smooth and discontinuous dynamics as well, which can be regarded as a rigid coupling of two separate SD oscillators vibrating horizontally. Complicated dynamical behaviors have been demonstrated with the coupled SD oscillator, such as the chaotic phenomenon for discontinuous cases [31], buckling phenomenon and co-dimension three bifurcation [32]. In 2015, a triple SD oscillator was proposed by Han et al. [33] consisting of a horizontal spring and two oblique springs in nonlinear geometrical configuration, which exhibits multiple-well dynamics for both smooth and discontinuous cases. High-order quasi-zero stiffness [34] can be built by this triple SD oscillator due to its nonlinear geometrical configuration, which is of great value in isolation engineering [35]. However, the phase structures and dynamical behaviors of the triple SD oscillator are not classified clearly and a series of problem about the heteroclinic bifurcation and the codimension-4 bifurcation has not been studied.

The first motivation of this paper is to investigate the complicated bifurcation of the triple SD oscillator, seen from [33], with a full picture of bifurcation sets including a heteroclinic bifurcation, phase portraits and the normal forms of the codimension-4 bifurcations [36–38]. The second motivation is to provide a theorem of structural stability of heteroclinic orbit [39–41] in 2-dimensional Hamilton system to obtain the heteroclinic bifurcation set. The third motivation is to present the complicated codimension-4 bifurcations including the closed orbit bifurcation, Hopf bifurcation, double Hopf bifurcation and also the homoclinic or heteroclinic bifurcations using subharmonic Melnikov functions by taking the normal form of one of the bifurcation surfaces as an example.

This paper is organized as follows. In Sect. 2, the mathematical model is built with governing equation and the Hamiltonian. In Sect. 3, the heteroclinic bifurcation condition is obtained by introducing a theorem of structural stability of heteroclinic orbit in Hamilton
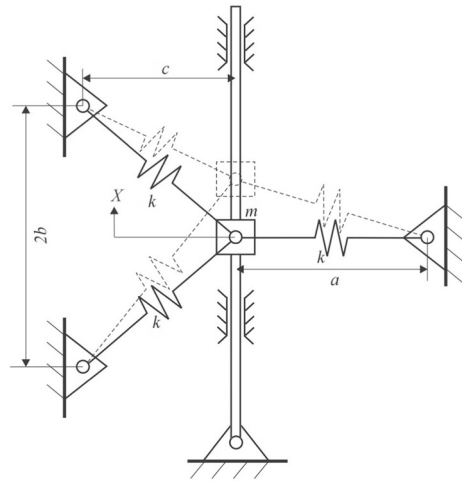
Fig. 1 Model of the triple SD oscillator [33]

system. In Sect. 4, the bifurcation sets are defined and studied, along with the complicated change of equilibria and the characteristics of restoring force, and the normal form of each bifurcation surface is built. In Sect. 5, the universal unfolding is obtained and the codimension-4 bifurcation is investigated by applying the subharmonic Melnikov function, taken one of the bifurcation surfaces as an example. Finally, the paper is closed with the summary of conclusions and the further challenges.

2 Mathematical model

Consider a model proposed in [33] based up on the SD oscillator [24], as shown in Fig. 1, consisting of a lumped mass m, a horizontal spring and two inclined springs pinned to rigid support.

Suppose the three springs are the same with stiffness k and initial length l, the horizontal distance on the left and right is c and a, respectively, and the vertical distance between the end points of the springs fixed to the rigid supports is $2b$. All the springs may be precompressed or pre-stretched depending on the value of a, b, c and l. The governing equation of free vibration can be written as

$$m\ddot{X} + kX\left(1 - \frac{l}{\sqrt{X^2 + a^2}}\right)$$
$$+ k(X + b)\left[1 - \frac{l}{\sqrt{(X + b)^2 + c^2}}\right]$$

$$+ k(X - b) \left[1 - \frac{l}{\sqrt{(X - b)^2 + c^2}} \right] = 0. \qquad (1)$$

The dimensionless form in 2-dimensional space can be obtained as shown in the following

$$\begin{cases} x' = y, \\ y' = -f(x, \alpha, \beta, \gamma), \end{cases} \qquad (2)$$

where $\omega_n = \sqrt{\frac{k}{m}}, x = \frac{X}{l}, \tau = \omega_n t, \alpha = \frac{a}{l}, \beta = \frac{b}{l}$ and $\gamma = \frac{c}{l}$, and $f(x, \alpha, \beta, \gamma)$ is the restoring force which can be written as

$$f(x, \alpha, \beta, \gamma) = 3x - \frac{x}{\sqrt{x^2 + \alpha^2}}$$
$$- \frac{x + \beta}{\sqrt{(x + \beta)^2 + \gamma^2}} - \frac{x - \beta}{\sqrt{(x - \beta)^2 + \gamma^2}}, \qquad (3)$$

System (2) is a Hamilton system whose Hamiltonian is $H(x, y) = \frac{1}{2}y^2 + V(x, \alpha, \beta, \gamma)$. $V(x, \alpha, \beta, \gamma)$ is the potential which can be written as

$$V(x, \alpha, \beta, \gamma) = \frac{1}{2} \left(\sqrt{x^2 + \alpha^2} - 1 \right)^2$$
$$+ \frac{1}{2} \left[\sqrt{(x + \beta)^2 + \gamma^2} - 1 \right]^2$$
$$+ \frac{1}{2} \left[\sqrt{(x - \beta)^2 + \gamma^2} - 1 \right]^2, \qquad (4)$$

3 Heteroclinic bifurcation of Hamilton system

The bifurcation condition of equilibriums of system (2) can be written as $f(x, \alpha, \beta, \gamma) = f'_x(x, \alpha, \beta, \gamma) = 0$. Heteroclinic orbits are usually structurally unstable, but some of them remains structurally stable for special cases in Hamilton systems. A heteroclinic orbit bifurcation of this system is discovered which is independent of equilibrium change.

Consider a 2-dimensional Hamilton system

$$\begin{cases} x' = \frac{\partial H}{\partial y}, \\ y' = -\frac{\partial H}{\partial x}, \end{cases} \qquad (5)$$

where the Hamiltonian $H : \mathbb{R}^2 \times \mathbb{R}^k \to \mathbb{R}$ which can be written as $H = H(x, y, \boldsymbol{p})$ is infinitely differentiable, which is independent of time τ, and $\boldsymbol{p} =$

$(p_1, p_2, \cdots, p_k)^{\mathrm{T}} \in \mathbb{R}^k$ is the parameter vector. The Jacobian matrix of system (5) is

$$J = \begin{bmatrix} \dfrac{\partial^2 H}{\partial x \partial y} & \dfrac{\partial^2 H}{\partial y^2} \\ -\dfrac{\partial^2 H}{\partial x^2} & -\dfrac{\partial^2 H}{\partial x \partial y} \end{bmatrix}, \qquad (6)$$

whose eigenvalue is $\lambda_{1,2} = \pm \sqrt{(\frac{\partial^2 H}{\partial x \partial y})^2 - \frac{\partial^2 H}{\partial x^2} \frac{\partial^2 H}{\partial y^2}}$.

To insure that system (5) has at least one heteroclinic orbit, it must be supposed that two saddle points with the same value of Hamiltonian exist, which indicates the condition of existence of a heteroclinic orbit as the following.

Condition 1:

$\exists (x_1, y_1), (x_2, y_2) \in \mathbb{R}^2$ and $\exists \boldsymbol{p} \in \mathbb{R}^k$, s.t. $H(x_1, y_1, \boldsymbol{p}) - H(x_2, y_2, \boldsymbol{p}) = 0, \frac{\partial H}{\partial x}|_{(x_l, y_l)} = \frac{\partial H}{\partial y}|_{(x_l, y_l)} = 0$ and $[(\frac{\partial^2 H}{\partial x \partial y})^2 - \frac{\partial^2 H}{\partial x^2} \frac{\partial^2 H}{\partial y^2}]|_{(x_l, y_l)} > 0, l = 1, 2.$

Here, a theorem to judge the structure stability of system (5) with heteroclinic orbit is given in the following with a brief proof.

Theorem 1 *Suppose condition 1 is satisfied for system (5) for a $\boldsymbol{p} \in \mathbb{R}^k$, which means (x_1, y_1) and (x_2, y_2) are saddles connected by a heteroclinic orbit. System (5) is structurally stable if $\forall i \in \{1, 2, \cdots, k\}$, s.t. $\frac{\partial H}{\partial p_i}|_{(x_1, y_1)} - \frac{\partial H}{\partial p_i}|_{(x_2, y_2)} \equiv 0$ in a small neighborhood near $\boldsymbol{p}$.*

Proof Assume that condition 1 is satisfied for a $\boldsymbol{p} \in \mathbb{R}^k$. We take a neighborhood of $\boldsymbol{p}$: $\Omega_{\boldsymbol{p}} = \{\tilde{\boldsymbol{p}}| \|\tilde{\boldsymbol{p}} - \boldsymbol{p}\| < \varepsilon, \varepsilon > 0\}$, and for simplification, it is assumed there is no equilibrium bifurcations in $\Omega_{\boldsymbol{p}}$. This indicates that for every $\tilde{\boldsymbol{p}} \in \Omega_{\boldsymbol{p}}$, there always exists the coordinates of a pair of saddle points $x_l = x_l(\tilde{\boldsymbol{p}}), y_l = y_l(\tilde{\boldsymbol{p}})$ ($l = 1, 2$) which are only dependent on parameter vector $\tilde{\boldsymbol{p}} \in \Omega_{\boldsymbol{p}}$, which means

$$\frac{\partial H}{\partial x}|_{(x_l, y_l)} = \frac{\partial H}{\partial y}|_{(x_l, y_l)} = 0,$$
$$\left[\left(\frac{\partial^2 H}{\partial x \partial y} \right)^2 - \frac{\partial^2 H}{\partial x^2} \frac{\partial^2 H}{\partial y^2} \right]|_{(x_l, y_l)} > 0,$$
$$l = 1, 2, \forall \tilde{\boldsymbol{p}} \in \Omega_{\boldsymbol{p}} \qquad (7)$$

Let $h(\tilde{\boldsymbol{p}}) = H(x_1(\tilde{\boldsymbol{p}}), y_1(\tilde{\boldsymbol{p}}), \tilde{\boldsymbol{p}}) - H(x_2(\tilde{\boldsymbol{p}}), y_2(\tilde{\boldsymbol{p}}), \tilde{\boldsymbol{p}})$. Certainly we have $h(\boldsymbol{p}) = 0$. System (5) with

heteroclinic orbit remaining structurally stable at $\boldsymbol{p}$ is equivalent to the fact that for every $\tilde{\boldsymbol{p}} \in \Omega_{\boldsymbol{p}}$, such that $h(\tilde{\boldsymbol{p}}) = 0$, which means $\nabla h(\tilde{\boldsymbol{p}}) = 0$.

Considering Eq. (7), the partial derivative of $h(\tilde{\boldsymbol{p}})$ with respect to p_i can be written as

$$
\begin{aligned}
\frac{\partial h}{\partial p_i} &= \frac{\partial H}{\partial x}\frac{\partial x_1}{\partial p_i} + \frac{\partial H}{\partial y}\frac{\partial y_1}{\partial p_i} \\
&\quad + \frac{\partial H}{\partial p_i} - \frac{\partial H}{\partial x}\frac{\partial x_2}{\partial p_i} - \frac{\partial H}{\partial y}\frac{\partial y_2}{\partial p_i} - \frac{\partial H}{\partial p_i} \\
&= \frac{\partial H}{\partial p_i}\big|_{(x_1,y_1)} - \frac{\partial H}{\partial p_i}\big|_{(x_2,y_2)} \qquad (i=1,2,\cdots,k)
\end{aligned}
$$

(8)

Thus, Theorem 1 is proved. To understand this theorem better, two examples of heteroclinic bifurcations are shown in appendix C. □

For a special kind of Hamilton system whose Hamiltonian can be written as $H(x, y, \boldsymbol{p}) = \frac{1}{2}y^2 + V(x, \boldsymbol{p})$, the theorem of structure stability with heteroclinic orbit can be simplified as follows:

Corollary 1 *For $H(x, y, \boldsymbol{p}) = \frac{1}{2}y^2 + V(x, \boldsymbol{p})$, system (5) is structurally stable with heteroclinic orbit if $\exists x_1, x_2 \in \mathbb{R}, \exists \boldsymbol{p} \in \mathbb{R}^k$, s.t. $V(x_1, \boldsymbol{p}) - V(x_2, \boldsymbol{p}) = 0$, $V_x'(x_l, \boldsymbol{p}) = 0$, $V_{xx}''(x_l, \boldsymbol{p}) < 0$, $l = 1, 2$; and $\forall i \in \{1, 2, \cdots, k\}$, s.t. $V_{p_i}'|_{x=x_1} - V_{p_i}'|_{x=x_2} \equiv 0$ in a small neighborhood near $\boldsymbol{p}$.*

For system (2), it is obvious that $V(-x, \boldsymbol{p}) = V(x, \boldsymbol{p})$, where $\boldsymbol{p} = (\alpha, \beta, \gamma)^{\mathrm{T}}$, and there are at most three saddles.

For the case of existing two saddles $(x_l, 0)$ ($l = 1, 2$), considering the symmetry, we have $x_2 = -x_1$ and $V_{p_i}'|_{x=x_1} - V_{p_i}'|_{x=x_2} = 0$ ($p_i = \alpha, \beta, \gamma$); thus, the system is structurally stable. But for the case of three saddles $(x_l, 0)$ ($l = 1, 2, 3, x_1 < x_2 < x_3$), we have $x_3 = -x_1, x_2 = 0$, and

$$
\begin{cases}
V_\alpha'|_{x=x_l} - V_\alpha'|_{x=0} = 1 - \dfrac{\alpha}{\sqrt{x_l^2 + \alpha^2}}, \\
V_\beta'|_{x=x_l} - V_\beta'|_{x=0} = \dfrac{2\beta}{\sqrt{\beta^2 + \gamma^2}} - \dfrac{x_l + \beta}{\sqrt{(x_l+\beta)^2 + \gamma^2}} + \dfrac{x_l - \beta}{\sqrt{(x_l-\beta)^2 + \gamma^2}}, \\
V_\gamma'|_{x=x_l} - V_\gamma'|_{x=0} = \dfrac{2\gamma}{\sqrt{\beta^2 + \gamma^2}} - \dfrac{\gamma}{\sqrt{(x_l+\beta)^2 + \gamma^2}} - \dfrac{\gamma}{\sqrt{(x_l-\beta)^2 + \gamma^2}},
\end{cases}
$$

(9)

where $l = 1, 3$. It is obvious that $V_\alpha'|_{x=x_l} - V_\alpha'|_{x=0} > 0$ for every $x_l \in \mathbb{R} \setminus \{0\}$ and every $\alpha \in \mathbb{R}$. Therefore, the conclusion of heteroclinic bifurcation of system (2) can be drawn as the following.

Corollary 2 *System (2) is structurally unstable with heteroclinic orbit if $\exists x_1, x_2 \in \mathbb{R} \setminus \{0\}$, $\exists \boldsymbol{p} \in \mathbb{R}^3$, s.t. $V(x_l, \boldsymbol{p}) - V(0, \boldsymbol{p}) = 0$, $V_x'(x_l, \boldsymbol{p}) = 0$, $V_{xx}''(x_l, \boldsymbol{p}) < 0$, $l = 1, 2$, where $\boldsymbol{p} = (\alpha, \beta, \gamma)^{\mathrm{T}}$.*

If the condition of Corollary 2 is satisfied, then we always have $V_\alpha'|_{x=x_l} - V_\alpha'|_{x=0} > 0$, which indicates the occurring of heteroclinic bifurcation.

4 Bifurcation sets and normal forms

4.1 Definition of bifurcation sets

According to Sect. 3, the bifurcation set can be obtained and written as

$$
\begin{aligned}
\Sigma = &\{(\alpha, \beta, \gamma) | f(x, \alpha, \beta, \gamma) = f_x'(x, \alpha, \beta, \gamma) = 0\} \\
&\cup \{(\alpha, \beta, \gamma) | V(x, \alpha, \beta, \gamma) = V(0, \alpha, \beta, \gamma), \\
&\quad V_x'(x, \alpha, \beta, \gamma) = 0, V_{xx}''(x, \alpha, \beta, \gamma) < 0\},
\end{aligned}
$$

(10)

which can be written in the following form

$$
\begin{aligned}
\Sigma = &B_1 \cup B_2 \cup B_3 \cup B_4 \cup B_5 \cup B_6 \\
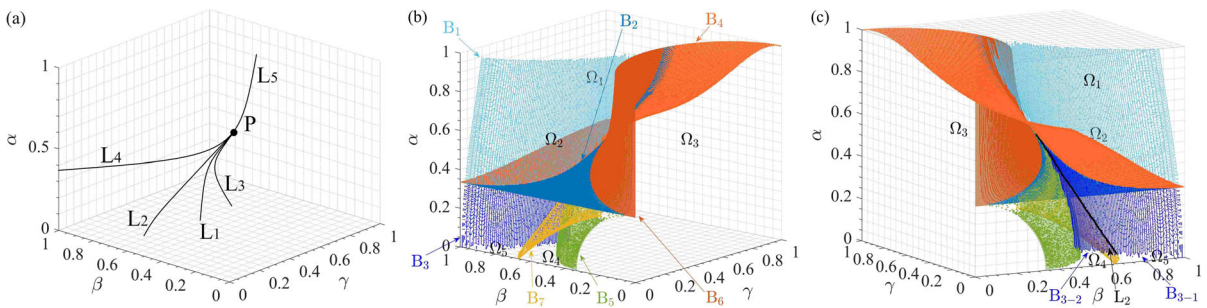&\cup B_7 \cup L_1 \cup L_2 \cup L_3 \cup L_4 \cup L_5 \cup P,
\end{aligned}
$$

(11)

where

$$
\begin{aligned}
B_1 = &\{(\alpha, \beta, \gamma) | C_1(\alpha, \beta, \gamma) > 0; \exists x_1 < 0 < x_2, \\
&f(x_i) = f'(x_i) = 0, i = 1, 2, f''(x_1) < 0 < f''(x_2)\}, \\
B_2 = &\{(\alpha, \beta, \gamma) | C_1(\alpha, \beta, \gamma) = 0; \\
&C_3(\alpha, \beta, \gamma) > 0; \exists x > 0, f(x) < 0\}, \\
B_3 = &\{(\alpha, \beta, \gamma) | C_1(\alpha, \beta, \gamma) < 0; \exists x_1 < 0 < x_2, \\
&f(x_i) = f'(x_i) = 0, i = 1, 2, f''(x_1) < 0 < f''(x_2)\}, \\
B_4 = &\{(\alpha, \beta, \gamma) | C_1(\alpha, \beta, \gamma) = 0; \\
&C_3(\alpha, \beta, \gamma) > 0; \forall x > 0, f(x) > 0\}, \\
B_5 = &\{(\alpha, \beta, \gamma) | C_1(\alpha, \beta, \gamma) < 0; \exists x_1 < 0 < x_2, \\
&f(x_i) = f'(x_i) = 0, i = 1, 2, f''(x_1) > 0 > f''(x_2)\}, \\
B_6 = &\{(\alpha, \beta, \gamma) | C_1(\alpha, \beta, \gamma) = 0; C_3(\alpha, \beta, \gamma) < 0\}, \\
B_7 = &\{(\alpha, \beta, \gamma) | C_1(\alpha, \beta, \gamma) < 0; \exists x_i, \\
&V(x_i) = V(0), V'(x_i) = 0, V''(x_i) < 0, i = 1, 2\},
\end{aligned}
$$

are all bifurcation surfaces of the first order,

$$
\begin{aligned}
L_1 = &\{(\alpha, \beta, \gamma) | C_1(\alpha, \beta, \gamma) < 0; \exists x_i, \\
&f(x_i) = f'(x_i) = f''(x_i) = 0, i = 1, 2\},
\end{aligned}
$$

Fig. 2 Bifurcation sets Σ in (α, β, γ) parameter space: **a.** catastrophe curves and the catastrophe point; **b.** bifurcation sets in front view; **c.** in dorsal view. (Bifurcation sets divide the (α, β, γ) plane into five persistent regions, marked Ω_1 to Ω_5, for which the corresponding phase portraits are persistent, on the boundaries B_1 to B_7, the portraits are nonpersistent)
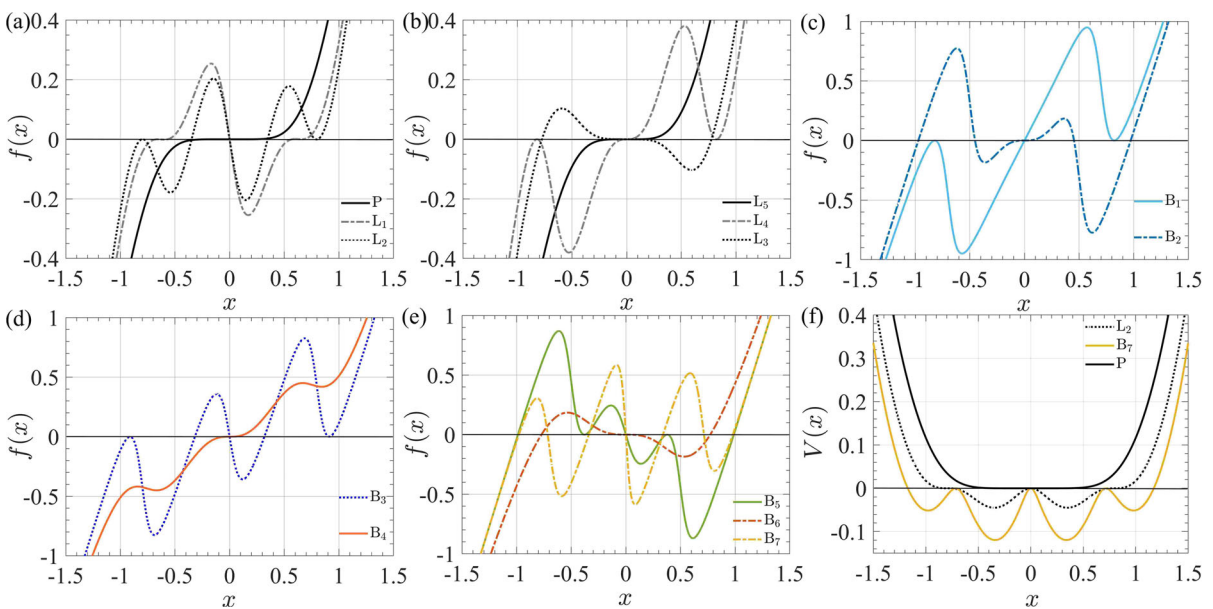
Fig. 3 Restoring force and potential energy for $\alpha > 0$ and $\gamma > 0$: **a.** restoring force for P, L_1, L_2; **b.** restoring force for L_3, L_4, L_5; **c.** restoring force for B_1, B_2; **d.** restoring force for B_3, B_4; **e.** restoring force for B_5, B_6, B_7; **(f).** potential energy for L_2, B_7, P

$L_2 = \{(\alpha, \beta, \gamma) | C_1(\alpha, \beta, \gamma) < 0; \exists x_1 < 0 < x_2,$
$V(x_i) = V(0), f(x_i) = f'(x_i) = 0, i = 1, 2\},$
$L_3 = \{(\alpha, \beta, \gamma) | C_1(\alpha, \beta, \gamma) = 0;$
$C_3(\alpha, \beta, \gamma) = 0; C_5(\alpha, \beta, \gamma) < 0\},$
$L_4 = \{(\alpha, \beta, \gamma) | C_1(\alpha, \beta, \gamma) = 0; \exists x_1 < 0 < x_2,$
$f(x_i) = f'(x_i) = 0, i = 1, 2, f''(x_1) < 0 < f''(x_2)\},$
$L_5 = \{(\alpha, \beta, \gamma) | C_1(\alpha, \beta, \gamma) = 0;$
$C_3(\alpha, \beta, \gamma) = 0; C_5(\alpha, \beta, \gamma) > 0\},$

are all catastrophe curves of the third order, and

$P = \{(\alpha, \beta, \gamma) | C_1(\alpha, \beta, \gamma) = 0; C_3(\alpha, \beta, \gamma) = 0;$
$C_5(\alpha, \beta, \gamma) = 0\} \approx (0.69967, 0.48105, 0.57721),$

is the catastrophe point of the fifth order, where $C_i(\alpha, \beta, \gamma) = \frac{f_x^{(i)}(0, \alpha, \beta, \gamma)}{i!}$ $(i = 1, 3, 5)$ is the Taylor expansion coefficient of the restoring force, which can be obtained as

Table 1 Equilibriums and stability of each set and each area, x_i, $(i = 1, 2, 3)$ has no analytical solution and $0 < x_1 < x_2 < x_3$

Bifurcation set/Area	Equilibriums
P, L$_5$, B$_4$	Stable degenerated center $(0, 0)$
L$_1$	Unstable saddle $(0, 0)$, Stable degenerated centers $(\pm x_1, 0)$
L$_2$	Unstable saddle $(0, 0)$, Stable centers $(\pm x_1, 0)$, unstable cuspidal saddles $(\pm x_2, 0)$
L$_3$, B$_6$	Unstable tangent saddle $(0, 0)$, stable centers $(\pm x_1, 0)$
L$_4$	Stable degenerated center $(0, 0)$, unstable cuspidal saddles $(\pm x_1, 0)$
B$_1$	Stable center $(0, 0)$, unstable cuspidal saddles $(\pm x_1, 0)$
B$_2$	Stable degenerated center $(0, 0)$, unstable saddles $(\pm x_1, 0)$, stable centers $(\pm x_2, 0)$
B$_3$	Unstable saddle $(0, 0)$, stable centers $(\pm x_1, 0)$, unstable cuspidal saddles $(\pm x_2, 0)$
B$_5$	Unstable saddle $(0, 0)$, unstable cuspidal saddles $(\pm x_1, 0)$, stable centers $(\pm x_2, 0)$
B$_7$	Unstable saddles $(0, 0)$ and $(\pm x_2, 0)$, stable centers $(\pm x_1, 0)$ and $(\pm x_3, 0)$
Ω_1	Stable center $(0, 0)$
Ω_2	Stable centers $(0, 0)$ and $(\pm x_2, 0)$, unstable saddles $(\pm x_1, 0)$
Ω_3	Unstable saddle $(0, 0)$, stable centers $(\pm x_1, 0)$
Ω_4, Ω_5	Unstable saddles $(0, 0)$ and $(\pm x_2, 0)$, stable centers $(\pm x_1, 0)$ and $(\pm x_3, 0)$

$$\begin{cases} C_1(\alpha, \beta, \gamma) = 3 - \dfrac{1}{\alpha} - \dfrac{2\gamma^2}{(\beta^2 + \gamma^2)^{\frac{3}{2}}}, \\ C_3(\alpha, \beta, \gamma) = \dfrac{1}{2\alpha^3} - \dfrac{\gamma^2(4\beta^2 - \gamma^2)}{(\beta^2 + \gamma^2)^{\frac{7}{2}}}, \\ C_5(\alpha, \beta, \gamma) = -\dfrac{3}{8\alpha^5} - \dfrac{3\gamma^2(8\beta^4 - 12\beta^2\gamma^2 + \gamma^4)}{4(\beta^2 + \gamma^2)^{\frac{11}{2}}}. \end{cases}$$

$$(12)$$

It is worth noticing that set B$_3$ is divided into B$_{3-1}$ and B$_{3-2}$ by set B$_7$, which is

$$B_{3-1} = \{(\alpha, \beta, \gamma) | (\alpha, \beta, \gamma) \in B_3; V(x_i) > V(0),$$
$$f(x_i) = f'(x_i) = 0, i = 1, 2\}$$
$$B_{3-2} = \{(\alpha, \beta, \gamma) | (\alpha, \beta, \gamma) \in B_3; V(x_i) < V(0),$$
$$f(x_i) = f'(x_i) = 0, i = 1, 2\}.$$

4.2 Structure of bifurcation sets

The bifurcation surfaces B$_i$, catastrophe curves L$_j$ and the catastrophe point P satisfy

$$\begin{cases} L_1 = \partial B_3 \cap \partial B_5 \setminus P, \quad L_2 = B_3 \cap \partial B_7 \setminus P, \\ L_3 = \partial B_2 \cap \partial B_6 \setminus P = \partial B_5 \cap \partial B_7 \setminus P, \\ L_4 = \partial B_1 \cap \partial B_3 \setminus P = \partial B_2 \cap \partial B_4 \setminus P, \\ L_5 = \partial B_4 \cap \partial B_6 \setminus P = \partial B_1 \cap \partial B_4 \setminus P, \\ P = \partial L_i \cap \partial L_j \quad (i \neq j). \end{cases}$$

$$(13)$$

where ∂B_i and ∂L_j represent the boundary of B$_i$ and L$_j$, respectively.

The important property shown in Eq. (13), which is proved in appendix B, indicates the structure of the bifurcation set Σ, as shown in Fig. 2 to provide a better understanding. The set Σ bifurcates at the catastrophe point P $\approx (0.69967, 0.48105, 0.57721)$ of the fifth order into five catastrophe curves L$_1 \sim$ L$_5$ of the third order and then into seven bifurcation surfaces B$_1 \sim$ B$_7$ of the first order. The surfaces are connected by the catastrophe curves: curve L$_1$ connects B$_3$ and B$_5$; L$_2$ connects B$_3$ and B$_7$; L$_3$ connects B$_2$, B$_5$, B$_6$ and B$_7$; L$_4$ connects B$_1$, B$_2$, B$_3$ and B$_4$; also, curve L$_5$ connects B$_1$, B$_4$ and B$_6$. The system exhibits different topological structure or dynamical behavior on each bifurcation surface and each catastrophe.

For $\alpha > 0$ and $\gamma > 0$, the system shows continuous dynamics (discontinuous cases are shown in appendix A) and the α-β-γ parameter space is divided into five areas named Ω_1 to Ω_5 by the bifurcation sets, as shown in Fig. 2b and Fig. 2c from the front view and dorsal view, respectively.

The restoring force $f(x)$ corresponding to the catastrophe point, the catastrophe curves and the bifurcation surfaces is plotted in Fig. 3. The restoring force $f(x)$ for L$_2$, L$_4$, B$_1$, B$_3$ and B$_5$ is all tangent to x-axis as there exists $x_i(i = 1, 2)$ that $f(x_i) = f'(x_i) = 0$, $f''(x_i) \neq 0$, and the restoring force for P, L$_1$, L$_3$, L$_4$, B$_2$ and B$_4$ exhibits stable quasi-zero stiffness, while the restoring

force for L_5 and B_6 exhibits unstable quasi-zero stiffness. This quasi-zero stiffness characteristics is of great value in isolation engineering.

The equilibriums and their stability of this system corresponding to each set and each area are shown in Table 1, which complicatedly changes as the varying of the three parameters, and the analytical solution cannot be obtained. The phase portraits corresponding to each set and each area are plotted in appendix A for different values of the Hamiltonian $H(x, y) = E$.

It is worth noticing that some high-order degenerated points are found as the varying of the three geometrical parameters, such as a 5th-order degenerated center at point P, a 3rd-order degenerated center at curve L_5 and a 1st-order degenerated center at the bifurcation surface B_4, which can be applied in engineering isolation. A pair of 1st-order degenerated center is found at curve L_1, curve L_4 and surface B_2. Meanwhile, a 3rd-order tangent saddle and a 1st-order tangent saddle are found at curve L_3 and surface B_6, respectively.

Multiple-well dynamics is also found on this system, such as a single well around by heteroclinic at L_4 and B_1, a double well at L_1, L_2, L_5, B_6 and Ω_3, triple well at Ω_2 and quadruple well at B_7.

4.3 Normal forms of bifurcation surfaces

The bifurcation diagrams for x versus β, α and γ with fixed (α, γ), (β, γ) and (α, β) are plotted in Fig. 4a, b and c, respectively, from which the type of bifurcation of each surface can be classified clearly. B_2 and B_4 are supercritical pitchfork bifurcation surfaces across which a stable center bifurcates into a pair of stable centers and an unstable saddle, changing through a degenerated center. But B_6 is subcritical pitchfork bifurcation surface across which an unstable saddle bifurcates into a pair of unstable saddles and a stable center, changing through a tangent saddle. B_1, B_3 and B_5 are sets of double saddle-node bifurcation across which a pair of stable centers and a pair of unstable saddles appear, changing through a pair of cuspidal saddles. B_7 is the set of heteroclinic bifurcation independent to equilibrium bifurcations.

The normal form of each bifurcation surface is shown in Table 2, along with the local bifurcation diagram and the changing of homoclinic or heteroclinic orbits. A pair of homoclinic orbits appears across the supercritical pitchfolk bifurcation set B_2 and B_4, and a

heteroclinic orbit appears across the subcritical pitchfolk bifurcation set B_6. The saddle-node bifurcation sets B_1 and B_{3-1} lead to a cuspidal heteroclinic orbit and the appearance of a pair of homoclinic orbits, but a cuspidal homoclinic orbit and the appearance of homoclinic orbits are led by saddle-center bifurcation set B_{3-2} and B_5.

5 Codimension-4 bifurcations

5.1 Universal unfolding and Subharmonic Melnikov function

The system can be written in the following form after Taylor expansion

$$
\begin{cases}
x' = y, \\
y' = -c_1(\alpha, \beta, \gamma)x - c_3(\alpha, \beta, \gamma)x^3 \\
\quad -c_5(\alpha, \beta, \gamma)x^5 - c_7(\alpha, \beta, \gamma)x^7,
\end{cases} \tag{14}
$$

where $c_i(\alpha, \beta, \gamma)$ $(i = 1, 3, 5, 7)$ is the coefficient of Taylor series of the restoring force.

We assume that the system is perturbed by a general van der Pol nonlinear damping, which leads to the forced dissipative oscillator as follows

$$
\begin{cases}
x' = y, \\
y' = -(\xi + \eta x^2 + \zeta x^4 + \nu x^6)y - c_1(\alpha, \beta, \gamma)x - c_3(\alpha, \beta, \gamma)x^3 \\
\quad -c_5(\alpha, \beta, \gamma)x^5 - c_7(\alpha, \beta, \gamma)x^7.
\end{cases} \tag{15}
$$

System (15) is the universal unfolding of system (14) which will be proved in another work. This system exhibits unfolded dynamics of three parameter codimension-four. Assuming $c_7(\alpha, \beta, \gamma) > 0$ and applying the scale transformation

$$
x \rightarrow \frac{c_7^{\frac{1}{6}}}{\nu^{\frac{1}{3}}}x, \quad \tau \rightarrow \frac{\nu}{c_7}\tau,
$$

a system equivalent to the nonlinear damped triple SD oscillator is obtained as follows

$$
\begin{cases}
x' = y, \\
y' = \mu_1 x + \mu_2 x^3 + \mu_3 x^5 + \mu_4 y \\
\quad +\mu_5 x^2 y + \mu_6 x^4 y - x^7 - x^6 y,
\end{cases} \tag{16}
$$
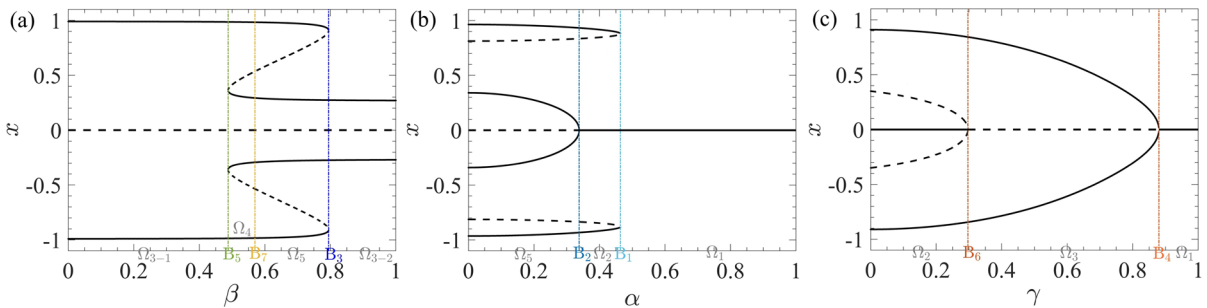
Fig. 4 Bifurcation diagrams for smooth cases: **a**. bifurcation diagram for x versus β for $\alpha = 0.2$ and $\gamma = 0.1$; **b**. bifurcation diagram for x versus α for $\beta = 0.764$ and $\gamma = 0.1$; **c**. bifurcation diagram for x versus γ for $\alpha = 0.85$ and $\beta = 0.35$

where $\mu_1 = -v^2 c_1 c_7^{-2}$, $\mu_2 = -v^{\frac{4}{3}} c_3 c_7^{-\frac{5}{3}}$, $\mu_3 = -v^{\frac{2}{3}} c_5 c_7^{-\frac{4}{3}}$, $\mu_4 = -\frac{\xi v}{c_7}$, $\mu_5 = -\frac{\eta v^{\frac{1}{3}}}{c_7^{\frac{2}{3}}}$ and $\mu_6 = -\frac{\zeta}{v^{\frac{1}{3}} c_7^{\frac{1}{3}}}$.

In order to study the global bifurcations for the corresponding homoclinic and heteroclinic orbits for three-parameter codimension-four bifurcation, a scale transformation is introduced as shown in the following

$$(x, y) \rightarrow (\delta^{n-1} x, \delta^n y), \quad \tau \rightarrow \frac{1}{\delta} \tau.$$

And let $\mu_1 = \mathrm{sgn}\mu_1 \delta^2$, $\mu_2 = -\delta^{4-2n} \varepsilon_1$, $\mu_3 = -\delta^{6-4n} \varepsilon_2$, $\mu_4 = \delta^2 \varepsilon_3$, $\mu_5 = \delta^{4-2n} \varepsilon_4$ and $\mu_6 = \delta^{6-4n} \varepsilon_5$, system (16) can be led to

$$\begin{cases} x' = y, \\ y' = \mathrm{sgn}\mu_1 x - \varepsilon_1 x^3 - \varepsilon_2 x^5 - x^7 \\ \quad + \delta(\varepsilon_3 + \varepsilon_4 x^2 + \varepsilon_5 x^4 - x^6)y, \end{cases} \quad (17)$$

while $n = \frac{4}{3}$.

For $\delta = 0$, system (17) is a Hamilton system

$$\begin{cases} x' = y, \\ y' = \mathrm{sgn}\mu_1 x - \varepsilon_1 x^3 - \varepsilon_2 x^5 - x^7, \end{cases} \quad (18)$$

whose Hamiltonian function can be obtained as

$$H(x, y) = \frac{1}{2} y^2 - \frac{\mathrm{sgn}\mu_1}{2} x^2 + \frac{\varepsilon_1}{4} x^4 + \frac{\varepsilon_2}{6} x^6 + \frac{1}{8} x^8. \quad (19)$$

The number of limit cycles of system (17) is related to the number of zero points of the subharmonic Melnikov function which can be obtained as follows

$$\begin{aligned} M(h) &= \int_0^T y^2(\tau)[\varepsilon_3 + \varepsilon_4 x^2(\tau) + \varepsilon_5 x^4(\tau) - x^6(\tau)]\mathrm{d}\tau \\ &= \int_{\Gamma(h)} y(\varepsilon_3 + \varepsilon_4 x^2 + \varepsilon_5 x^4 - x^6)\mathrm{d}x, \end{aligned} \quad (20)$$

where $\Gamma(h) = \{(x, y)|H(x, y) = h\}$ and T is the period of curve $\Gamma(h)$.

It is clear that the above subharmonic Melnikov function can be used to deprive all the bifurcations corresponding to the normal forms in Table 1. For example, when $\varepsilon_1 > 0$ and $\varepsilon_2 < -2\sqrt{\varepsilon_1}$, for B$_2$, when $\mu_1 > 0$, $\varepsilon_1 = \epsilon_1 - \lambda$ and $\varepsilon_2 = \epsilon_2$, for B$_{3-1}$ and B$_{3-2}$, and also the complicated bifurcation corresponding to normal form of B$_5$ and B$_7$ can be shown if the parameters $\mu_1 > 0$, $\varepsilon_1 = \epsilon_1 + \lambda$ and $\varepsilon_2 = \epsilon_2$ are taken.

Due to the limited space, only the codimension bifurcations for B$_2$ are presented in the following parts, that is, $\varepsilon_1 > 0$ and $\varepsilon_2 < -2\sqrt{\varepsilon_1}$. For the convenience, $\mu_1 \in \mathbb{R}$ is assumed and $\varepsilon_1 = 5.5$, $\varepsilon_2 = -5$ is taken in the following analysis.

For $\mu_1 < 0$, $\Gamma(h)$ is classified to three types of periodic orbits as shown in Fig. 5a: $\Gamma_1(h)$ for $0 < h < h_2$, $\Gamma_2(h)$ for $h_1 < h < h_2$ and $\Gamma_3(h)$ for $h > h_2$, while $\Gamma(h_2)$ is the homo-heteroclinic orbits. $h_1 \approx 1.47881$ and $h_2 \approx 1.83333$ are the potential energy at the equilibriums of system (18) for $\mu_1 < 0$.

For $\mu_1 > 0$, $\Gamma(h)$ is classified to four types of periodic orbits as shown in Fig. 5c: $\Gamma_4(h)$ for $h_3 < h < h_4$, $\Gamma_5(h)$ for $h_4 < h < 0$, $\Gamma_6(h)$ for $0 < h < h_5$ and $\Gamma_7(h)$ for $h > h_5$, while $\Gamma(0)$ is the double-homoclinic orbits and $\Gamma(h_5)$ is the homo-heteroclinic orbits. $h_3 \approx -1.87814$, $h_4 \approx -0.05206$ and $h_5 \approx 0.20104$ are the

Table 2 Normal forms corresponding to the bifurcation surfaces

surface	normal form	diagram	orbit bifurcation
B_1	$-x + \lambda x^3 + 2x^3 - x^5$		
B_2	$\lambda x - \epsilon_1 x^3 - \epsilon_2 x^5 - x^7$, where $\epsilon_1 > 0$, $\epsilon_2 < -2\sqrt{\epsilon_1}$		
B_{3-1}	$x + \lambda x^3 - \epsilon_1 x^3 - \epsilon_2 x^5 - x^7$, where $27 + 9\epsilon_1 \epsilon_2 - 2\epsilon_2^3$ $+2(\epsilon_2^2 - 3\epsilon_1)^{\frac{3}{2}} = 0$, $3 < \epsilon_1 < 3.7798$		
B_{3-2}	$x + \lambda x^3 - \epsilon_1 x^3 - \epsilon_2 x^5 - x^7$, where $27 + 9\epsilon_1 \epsilon_2 - 2\epsilon_2^3$ $+2(\epsilon_2^2 - 3\epsilon_1)^{\frac{3}{2}} = 0$, $\epsilon_1 > 3.7798$		
B_4	$\lambda x - x^3$		
B_5	$x - \lambda x^3 - \epsilon_1 x^3 - \epsilon_2 x^5 - x^7$, where $27 + 9\epsilon_1 \epsilon_2 - 2\epsilon_2^3$ $-2(\epsilon_2^2 - 3\epsilon_1)^{\frac{3}{2}} = 0$, $\epsilon_1 > 3$, $\epsilon_2 < -3$		
B_6	$-\lambda x + \epsilon x^3 - x^5$, where $\epsilon > 0$		
B_7	$x - \lambda x^3 - \epsilon_1 x^3 - \epsilon_2 x^5 - x^7$, where $81 + 18\epsilon_1 \epsilon_2 - \frac{32}{9}\epsilon_2^3$ $+\frac{\sqrt{2}}{9}(8\epsilon_2^2 - 27\epsilon_1)^{\frac{3}{2}} = 0$, $\epsilon_1 > 3$, $\epsilon_2 < -3$		

potential energy at the equilibriums of system (18) for $\mu_1 > 0$.

For $\mu_1 = 0$, $\Gamma(h)$ is classified to three types of periodic orbits as shown in Fig. 5b: $\Gamma_8(h)$ for $0 < h < h_7$, $\Gamma_9(h)$ for $h_6 < h < h_7$ and $\Gamma_{10}(h)$ for $h > h_7$, while $\Gamma(h_7)$ is the homo-heteroclinic orbits. $h_6 \approx -0.15585$ and $h_7 \approx 0.92668$ are the potential energy at the equilibriums of system (18) for $\mu_1 = 0$.

Let

$$I_n^i(h) = \int_{\Gamma_i(h)} x^{2n} y \, dx, \quad P_n^i(h) = \frac{I_n^i(h)}{I_0^i(h)},$$

and $p_i(h) = P_3^i(h) - \varepsilon_5 P_2^i(h) - \varepsilon_4 P_1^i(h)$. The zero points of function $M(h)$ can be regarded as the intersections of curve $p = p_i(h)$ and line $p = \varepsilon_3$.
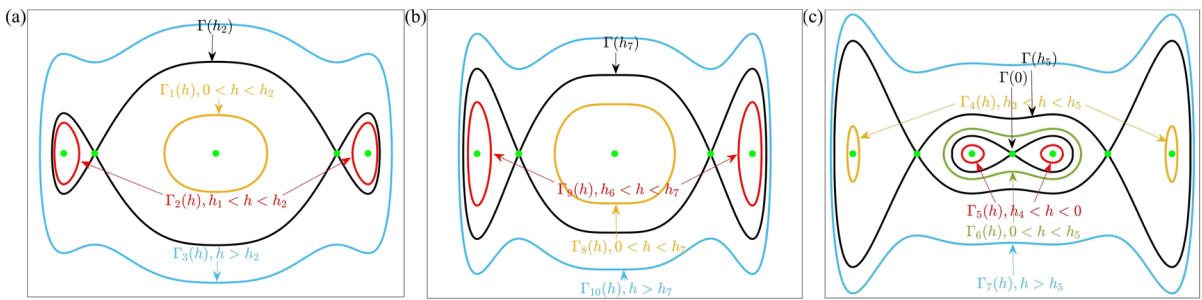
Fig. 5 Different types of orbit $\Gamma(h) = \{(x, y)|H(x, y) = h\}$ of system (18) for $\varepsilon_1 = 5.5, \varepsilon_2 = -5$: **a**. $\mu_1 < 0$; **b**. $\mu_1 = 0$; **c**. $\mu_1 > 0$

5.2 Jacobian matrix and eigenvalues

To classify the equilibriums, the Jacobian matrix of system (17) is obtained as follows

$$J = \begin{bmatrix} 0 & 1 \\ -f'(x_i) & \delta(\varepsilon_3 + \varepsilon_4 x_i^2 + \varepsilon_5 x_i^4 - x_i^6) \end{bmatrix}, \quad (21)$$

where $f'(x) = -\text{sgn}\mu_1 + 3\varepsilon_1 x^2 + 5\varepsilon_2 x^4 + 7x^6$ is the stiffness and $(x_i, 0)$ is one of the equilibriums. The eigenvalues can be written as

$$\lambda_{1,2} = \frac{1}{2}[\delta(\varepsilon_3 + \varepsilon_4 x_i^2 + \varepsilon_5 x_i^4 - x_i^6) \\ \pm \sqrt{\delta^2(\varepsilon_3 + \varepsilon_4 x_i^2 + \varepsilon_5 x_i^4 - x_i^6)^2 - 4f'(x_i)}]. \quad (22)$$

For the equilibrium $(x_i, 0)$ being saddle point $(f'(x_i) < 0)$ without perturbation $(\delta = 0)$, the eigenvalues $\lambda_{1,2}$ under perturbation $(\delta > 0)$ are a pair of real numbers being positive and negative, respectively, implying that $(x_i, 0)$ for $f'(x_i) < 0$ is always a saddle point for every ε_3, ε_4 and ε_5.

For the equilibrium $(x_i, 0)$ being center point $(f'(x_i) > 0)$ without perturbation $(\delta = 0)$, the conclusion is more complicated under perturbation $(\delta > 0)$. $(x_i, 0)$ is stable node when $\varepsilon_3 < -\frac{2\sqrt{f'(x_i)}}{\delta} - \varepsilon_4 x_i^2 - \varepsilon_5 x_i^4 + x_i^6$, stable degenerated node when $\varepsilon_3 = -\frac{2\sqrt{f'(x_i)}}{\delta} - \varepsilon_4 x_i^2 - \varepsilon_5 x_i^4 + x_i^6$, stable focus when $-\frac{2\sqrt{f'(x_i)}}{\delta} - \varepsilon_4 x_i^2 - \varepsilon_5 x_i^4 + x_i^6 < \varepsilon_3 < -\varepsilon_4 x_i^2 - \varepsilon_5 x_i^4 + x_i^6$, center point when $\varepsilon_3 = -\varepsilon_4 x_i^2 - \varepsilon_5 x_i^4 + x_i^6$, unstable focus when $-\varepsilon_4 x_i^2 - \varepsilon_5 x_i^4 + x_i^6 < \varepsilon_3 < \frac{2\sqrt{f'(x_i)}}{\delta} - \varepsilon_4 x_i^2 - \varepsilon_5 x_i^4 + x_i^6$, unstable degenerated node $\varepsilon_3 = \frac{2\sqrt{f'(x_i)}}{\delta} - \varepsilon_4 x_i^2 - \varepsilon_5 x_i^4 + x_i^6$, unstable node $\varepsilon_3 > \frac{2\sqrt{f'(x_i)}}{\delta} - \varepsilon_4 x_i^2 - \varepsilon_5 x_i^4 + x_i^6$.

5.3 Codimension-4 bifurcations

For the next analysis, it is assumed that $\varepsilon_1 = 5.5, \varepsilon_2 = -5, \varepsilon_4 = -1, \varepsilon_5 = 3.6$ and $\delta = 0.4$.

5.3.1 Equilibrium change

For $\mu_1 < 0$, equilibrium $(\pm 1.41421, 0)$ is a pair of saddles for every ε_3, while equilibriums $(0, 0)$ and $(\pm 1.77716, 0)$ are listed in Table 3 for different ε_3. For $\mu_1 > 0$, equilibriums $(0, 0)$ and $(\pm 1.12104, 0)$ are saddles for every ε_3, while equilibriums $(\pm 0.47565, 0)$ and $(\pm 1.87537, 0)$ are listed in Table 4 for different ε_3.

5.3.2 Limit cycle bifurcations

The curves of $p_i(h)$ for both $\mu_1 > 0$, $\mu_1 < 0$ and $\mu_1 = 0$ are calculated by numerical integration method and shown in Fig. 6 and the bifurcation diagram on $\mu_1-\mu_4$ plane can be obtained by using the transformation $\mu_1 = \text{sgn}\mu_1\delta^2$, $\mu_4 = \delta^2\varepsilon_3$. The bifurcation sets shown in Fig. 7a can be described as follows:

$$B_I = \{\mu_4 = c_1\mu_1, \mu_1 < 0\},$$
$$H_1 = \{\mu_4 = c_2\mu_1, \mu_1 < 0\},$$
$$HL_I = \{\mu_4 = c_3\mu_1, \mu_1 < 0\},$$
$$HL_{II} = \{\mu_4 = c_4\mu_1, \mu_1 < 0\},$$
$$B_{II} = \{\mu_4 = c_5\mu_1, \mu_1 < 0\},$$
$$H_{2I} = \{\mu_4 = c_6\mu_1, \mu_1 < 0\},$$
$$HL_{III} = \{\mu_4 = c_7\mu_1, \mu_1 < 0\},$$
$$H_{2II} = \{\mu_4 = c_8\mu_1, \mu_1 > 0\},$$
$$HL_{IV} = \{\mu_4 = c_9\mu_1, \mu_1 > 0\},$$
$$HL_V = \{\mu_4 = c_{10}\mu_1, \mu_1 > 0\},$$
$$B_{III} = \{\mu_4 = c_{11}\mu_1, \mu_1 > 0\},$$

Table 3 Equilibrium change for $\mu_1 < 0$

Equilibrium	$(0, 0)$	$(\pm1.77716, 0)$
Stable node	$\varepsilon_3 < -5$	$\varepsilon_3 < -25.8776$
Stable degenerated node	$\varepsilon_3 = -5$	$\varepsilon_3 = -25.8776$
Stable focus	$-5 < \varepsilon_3 < 0$	$-25.8776 < \varepsilon_3 < -1.2476$
Center point	$\varepsilon_3 = 0$	$\varepsilon_3 = -1.2476$
Unstable focus	$0 < \varepsilon_3 < 5$	$-1.2476 < \varepsilon_3 < 23.3824$
Unstable degenerated node	$\varepsilon_3 = 5$	$\varepsilon_3 = 23.3824$
Unstable node	$\varepsilon_3 > 5$	$\varepsilon_3 > 23.3824$

Table 4 Equilibrium change for $\mu_1 > 0$

Equilibrium	$(\pm0.47565, 0)$	$(\pm1.87537, 0)$
Stable node	$\varepsilon_3 < -6.1400$	$\varepsilon_3 < -33.6755$
Stable degenerated node	$\varepsilon_3 = -6.1400$	$\varepsilon_3 = -33.6755$
Stable focus	$-6.1400 < \varepsilon_3 < 0.0536$	$-33.6755 < \varepsilon_3 < 2.4905$
Center point	$\varepsilon_3 = 0.0536$	$\varepsilon_3 = 2.4905$
Unstable focus	$0.0536 < \varepsilon_3 < 6.2471$	$2.4905 < \varepsilon_3 < 38.6565$
Unstable degenerated node	$\varepsilon_3 = 6.2471$	$\varepsilon_3 = 38.6565$
Unstable node	$\varepsilon_3 > 6.2471$	$\varepsilon_3 > 38.6565$

Fig. 6 **a**. The curve of function $p(h)$ for $\mu_1 < 0$; **b**. the curve of function $p(h)$ for $\mu_1 > 0$; **c**. detail of the gray box in figure b; **d**. the curve of function $p(h)$ for $\mu_1 = 0$
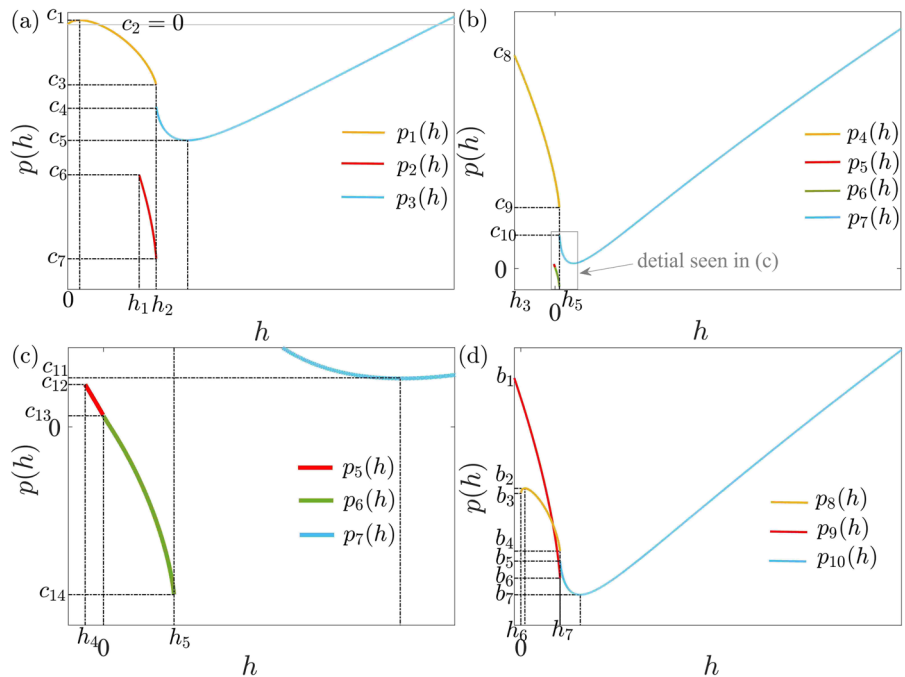
$H_{2III} = \{\mu_4 = c_{12}\mu_1, \mu_1 > 0\}$,

$HL_{VI} = \{\mu_4 = c_{13}\mu_1, \mu_1 > 0\}$,

$HL_{VII} = \{\mu_4 = c_{14}\mu_1, \mu_1 > 0\}$,

where $c_1 \approx 0.03737$, $c_2 = 0$, $c_3 \approx -0.50463$, $c_4 \approx -0.84214$, $c_5 \approx -0.95882$, $c_6 \approx -1.242$, $c_7 \approx -1.93395$, $c_8 = 2.5$, $c_9 \approx 0.82500$, $c_{10} \approx 0.33091$, $c_{11} \approx 0.17889$, $c_{12} \approx 0.056$, $c_{13} \approx 0.01413$ and $c_{14} \approx -0.21213$. The bifurcation sets divide the $\mu_1 - \mu_4$ plane into sixteen areas, named I to XVI.

It is worth noticing that the limit cycle bifurcation also happens while $\mu_1 \equiv 0$, dividing line $\mu_1 = 0$ into eight parts, which can be described as the following:

$O_I = \{\mu_4 > \delta^2 b_1, \mu_1 = 0\}$,

$L_1 = \{\delta^2 b_2 < \mu_4 < \delta^2 b_1, \mu_1 = 0\}$,

$L_2 = \{\delta^2 b_3 < \mu_4 < \delta^2 b_2, \mu_1 = 0\}$,

$L_3 = \{\delta^2 b_4 < \mu_4 < \delta^2 b_3, \mu_1 = 0\}$,

$L_4 = \{\delta^2 b_5 < \mu_4 < \delta^2 b_4, \mu_1 = 0\}$,

$L_5 = \{\delta^2 b_6 < \mu_4 < \delta^2 b_5, \mu_1 = 0\}$,

$L_6 = \{\delta^2 b_7 < \mu_4 < \delta^2 b_6, \mu_1 = 0\}$,

$O_{II} = \{\mu_4 < \delta^2 b_7, \mu_1 = 0\}$,

where $b_1 \approx 0.71441$, $b_2 = 0.03832$, $b_3 = 0$, $b_4 \approx -0.34552$, $b_5 \approx -0.43164$, $b_6 \approx -0.46325$ and $b_7 \approx -0.59598$.

As shown in Fig. 5, Γ_1, Γ_3, Γ_6, Γ_7, Γ_8 and Γ_{10} all represent a single periodic orbit for a constant h, so each intersection of $p = \varepsilon_3$ and $p = p_i(h)$ ($i = 1, 3, 6, 7, 8, 10$) corresponds to a single limit cycle. Similarly, each intersection of $p = \varepsilon_3$ and $p = p_i(h)$ ($i = 2, 4, 5, 9$) corresponds to a pair of limit cycles because Γ_2, Γ_4, Γ_5 and Γ_9 all represent a pair of periodic orbits. $\Gamma(h_2)$ for $\mu_1 < 0$, $\Gamma(0)$ and $\Gamma(h_5)$ for $\mu_1 > 0$, $\Gamma(h_7)$ for $\mu_1 = 0$ are all homoclinic or heteroclinic orbits, implying that $p_i(h_2)$ for $\mu_1 < 0$, $p_i(0)$, $p_i(h_5)$ for $\mu_1 > 0$ and $p_i(h_7)$ for $\mu_1 = 0$ correspond to homoclinic or heteroclinic bifurcation. Thus, the conclusion can be drawn as the following:
(1) closed orbit bifurcation set: B_I, B_{II}, $B_{III}(\varepsilon_3 = c_1, c_5, c_{11})$, where a semi-stable limit cycle bifurcates into a stable one and an unstable one;
(2) Hopf bifurcation set: $H_1(\varepsilon_3 = c_2)$;
(3) double Hopf bifurcation set: H_{2I}, H_{2II}, $H_{2III}(\varepsilon_3 = c_6, c_8, c_{12})$;

(4) homoclinic or heteroclinic bifurcation set: HL_I, HL_{II}, HL_{III}, HL_{IV}, HL_V, HL_{VI}, $HL_{VII}(\varepsilon_3 = c_3, c_4, c_7, c_9, c_{10}, c_{13}, c_{14})$, where limit cycle turns into homoclinic or heteroclinic orbit;
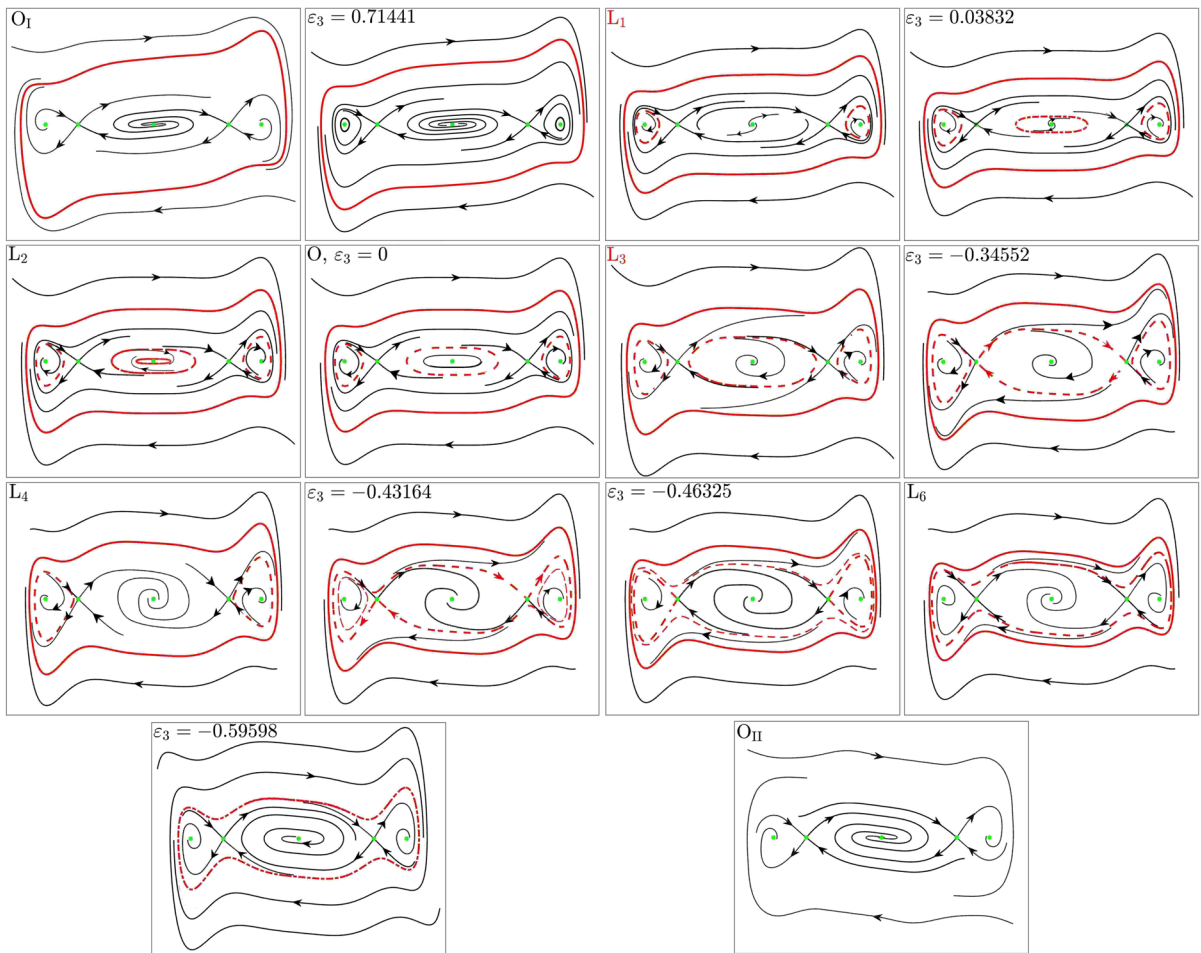(5) supercritical pitchfolk equilibrium bifurcation set: O_I, O_{II}.

The phase portraits are shown in Fig. 8, 9 and 10 for $\mu_1 < 0$, $\mu_1 = 0$ and $\mu_1 > 0$, respectively, corresponding to each area and each bifurcation set in Fig. 7.

6 Conclusion and discussions

The complicated bifurcations of a nonlinear oscillator consisting of a horizontal spring and two oblique springs in nonlinear geometrical configuration governed by three geometrical parameters have been studied in this paper. The bifurcation sets have been defined according to the characteristics of restoring force and potential, including bifurcation surfaces, catastrophe curves of the first and third order, and also a catastrophe point of the fifth order. A special kind of heteroclinic bifurcation of this oscillator is discovered by investigating the structural stability of heteroclinic orbits in Hamilton system. The phase portraits, multiple-well potential energy and force-displacement characteristics have been investigated, demonstrating high-order singulars and multiple-well dynamics. Complex bifurcations have been demonstrated in smooth region with the normal form of each bifurcation surface, classified as supercritical pitchfolk bifurcation, subcritical pitchfolk bifurcation and double saddle-center bifurcation. Subharmonic Melnikov function has been employed to detect the complicated bifurcations of limit cycles including closed orbit bifurcation, Hopf bifurcation, double Hopf bifurcation and homoclinic or hetero-

Fig. 7 **a**. bifurcation diagram on $\mu_1 - \mu_4$ plane; **b**. detail of the gray box in figure a, the bifurcation for $\mu_1 = 0$ for detail

Fig. 8 Phase portraits of system (17) for $\mu_1 < 0$, $\varepsilon_1 = 5.5$, $\varepsilon_2 = -5$, $\varepsilon_4 = -1$ and $\varepsilon_5 = 3.6$ ($\delta = 0.4$, green points represent equilibrium points and red lines represent limit cycles)

Fig. 9 Phase portraits of system (17) for $\mu_1 = 0$, $\varepsilon_1 = 5.5$, $\varepsilon_2 = -5$, $\varepsilon_4 = -1$ and $\varepsilon_5 = 3.6$ ($\delta = 0.4$, green points represent equilibrium points and red lines represent limit cycles)
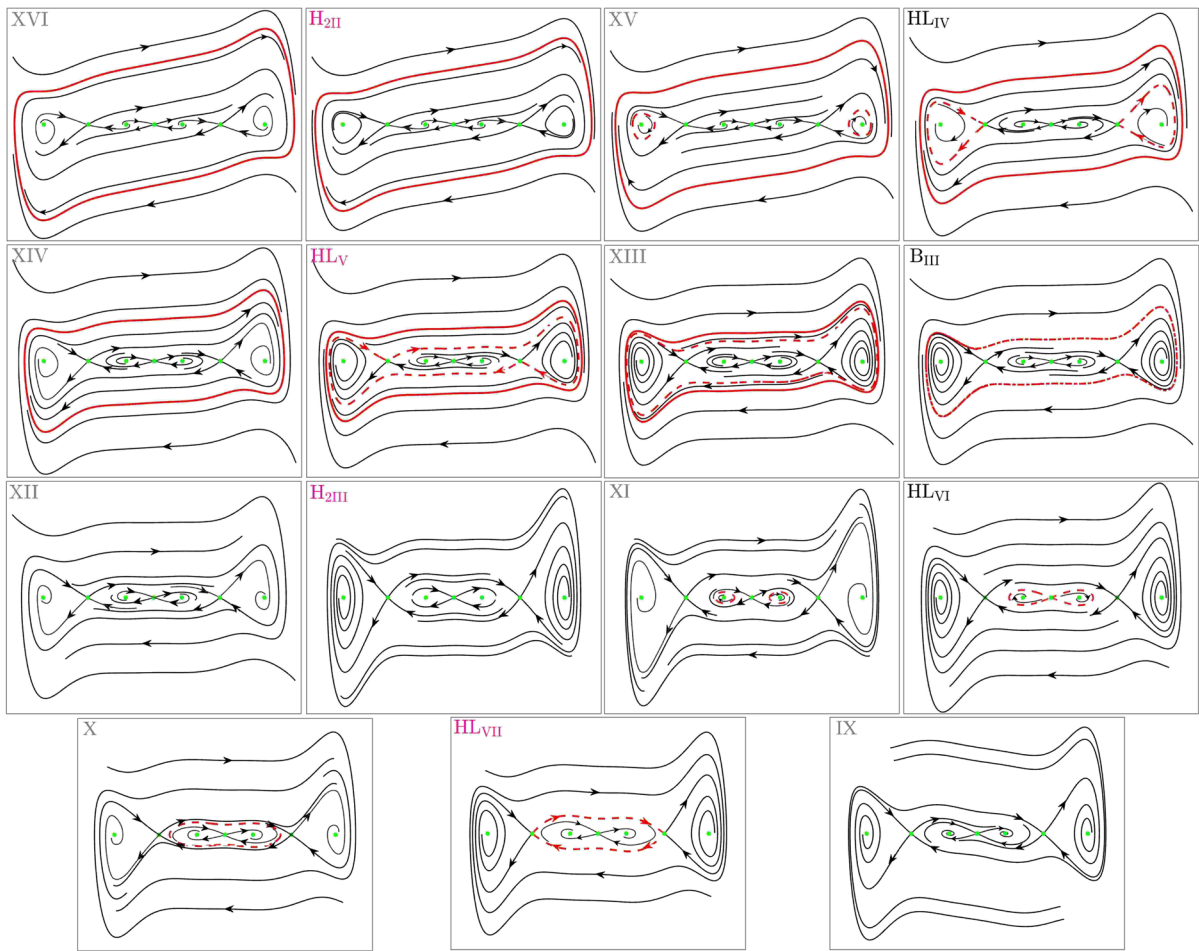
Fig. 10 Phase portraits of system (17) for $\mu_1 > 0$, $\varepsilon_1 = 5.5$, $\varepsilon_2 = -5$, $\varepsilon_4 = -1$ and $\varepsilon_5 = 3.6$ ($\delta = 0.4$, green points represent equilibrium points and red lines represent limit cycles)

clinic bifurcations, taken bifurcation surface B_2 as an example. The codimension-4 bifurcation of the triple SD oscillator corresponding to other normal forms will be investigated in another paper. Also, further researches can be undertaken to analyze for the complicated behaviors of this oscillator such as resonant behaviors [42,43] and the chaotic behaviors [44–46] under the external perturbations as well.

Author contributions All authors contributed to the study conception and design; all authors read and approved the final manuscript.

Declarations

Conflict of interest The authors declare that they have no conflict of interest.
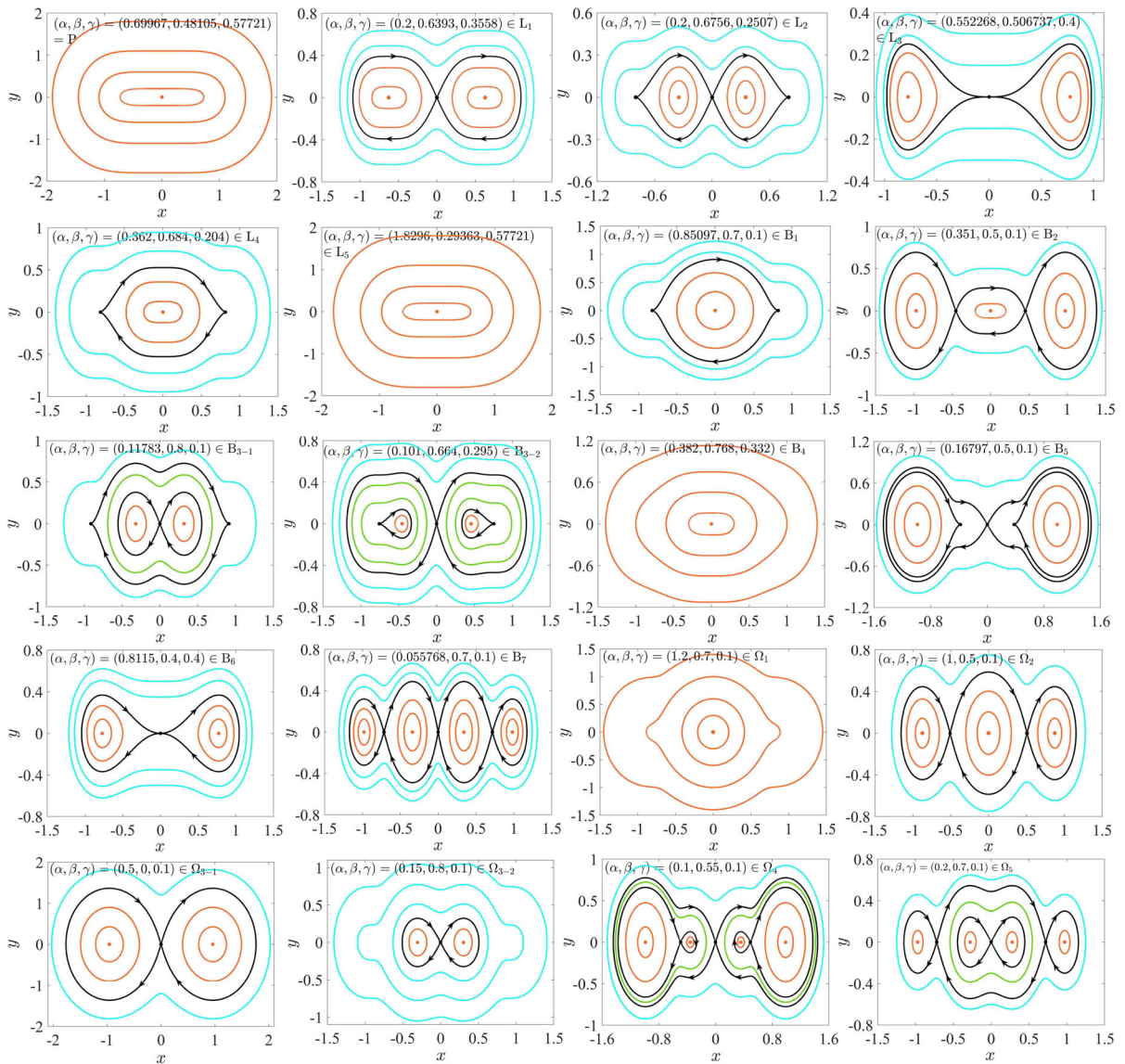
Fig. 11 Phase portraits for $\alpha > 0$ and $\gamma > 0$ with a catastrophe point, 5 catastrophe curves, 7 bifurcation surfaces and 5 areas (The value of parameters and the belonged set are shown in each figure legend)

A Phase structures

A.1 Smooth cases

Phase portraits of smooth case for $\alpha > 0$ and $\gamma > 0$ are plotted in Fig. 11. Orange lines represent small periodic orbits, green and blue lines represent large periodic orbits which encircle heteroclinic or homoclinic orbits, and black lines represent heteroclinic or homoclinic orbits.

A.2 Discontinuous cases

For $\alpha = 0$ and $\gamma > 0$, only $x = 0$ is discontinuous. The restoring force can be written as $f(x, 0, \beta, \gamma) = 3x - \mathrm{sgn}x - \dfrac{x + \beta}{\sqrt{(x + \beta)^2 + \gamma^2}} - \dfrac{x - \beta}{\sqrt{(x - \beta)^2 + \gamma^2}}$. The bifurcation diagram along with the bifurcation sets is shown in Fig. 12. And the phase portraits corresponding to each set and each area are shown in Fig. 13.
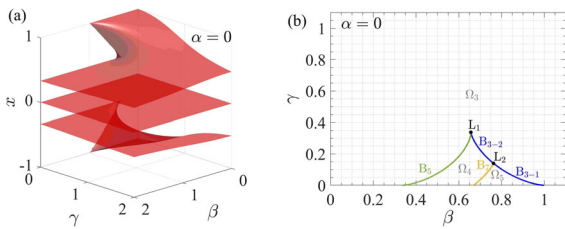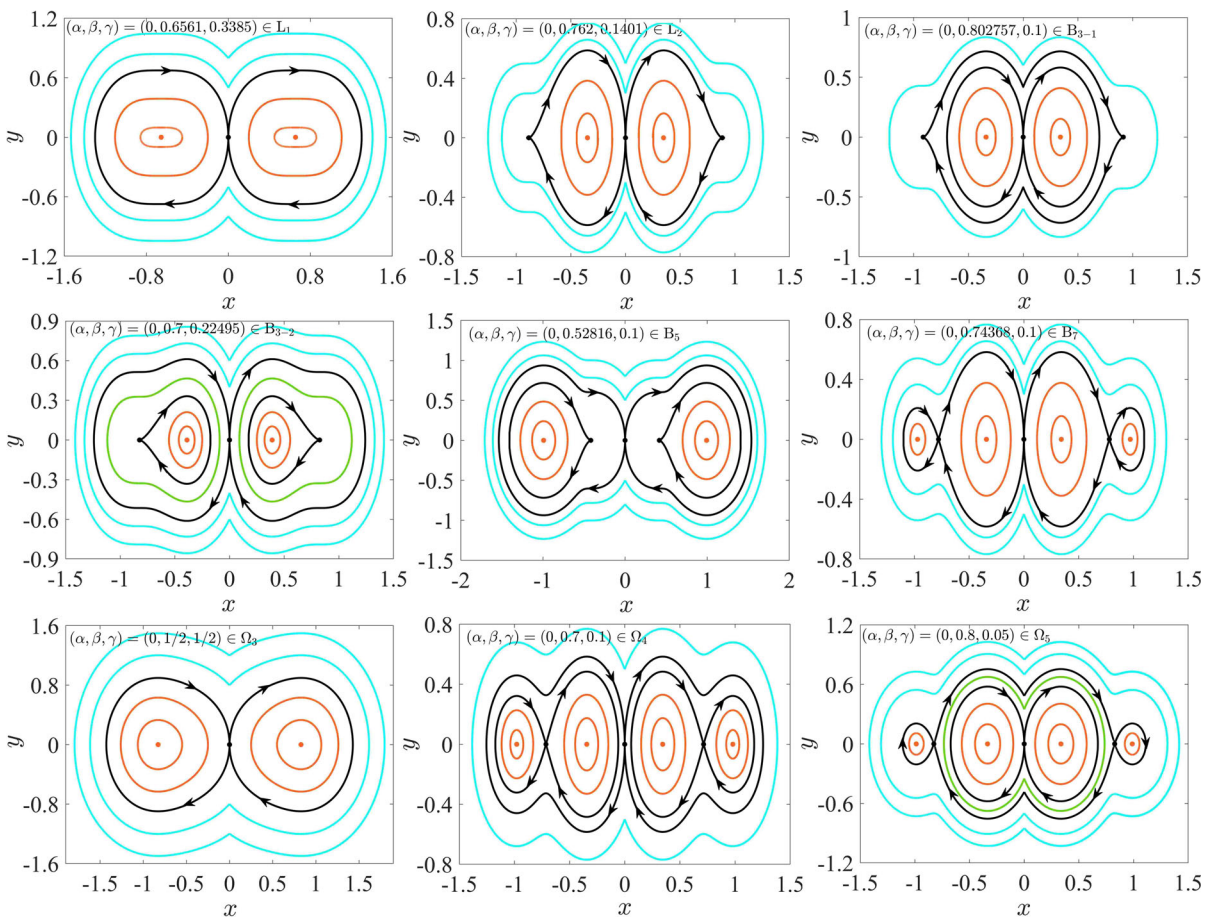
Fig. 12 Bifurcation diagrams for $\alpha = 0$: **a**. equilibrium bifurcation surfaces; **b**. bifurcation sets on β-γ plane. (Bifurcation sets divide the (β, γ) plane into three persistent regions, marked Ω_3, Ω_4 and Ω_5, for which the corresponding phase portraits are persistent, on the boundaries B_{3-1}, B_{3-2}, B_5 B_7, the portraits are nonpersistent)

β). The bifurcation diagram along with the bifurcation sets is shown in Fig. 14. The corresponding phase portraits are shown in Fig. 15.

For $\alpha = 0$, $\beta > 0$ and $\gamma = 0$, $x = 0$, $x = \beta$ and $x = -\beta$ are all discontinuous. The restoring force can be written as $f(0, \beta, 0) = 3x - \text{sgn}x - \text{sgn}(x + \beta) - \text{sgn}(x - \beta)$. The bifurcation diagram is shown in Fig. 16 for x versus β. The phase portraits are plotted in Fig. 17.

For $\alpha > 0$, $\beta > 0$ and $\gamma = 0$, $x = \beta$ and $x = -\beta$ are discontinuous. The restoring force can be written as
$$f(x, \alpha, \beta, 0) = -\frac{x}{\sqrt{x^2 + \alpha^2}} - \text{sgn}(x + \beta) - \text{sgn}(x -$$

Fig. 13 Phase portraits for $\alpha = 0$ (The value of parameters and the belonged set are shown in each figure legend)

Fig. 14 Bifurcation diagrams for $\gamma = 0$: **a**. equilibrium bifurcation surfaces; **b**. bifurcation sets on α-β plane. (Bifurcation sets divide the (α, β) plane into five persistent regions, marked Ω_1 to Ω_5, for which the corresponding phase portraits are persistent, on the boundaries B_1 to B_7, the portraits are nonpersistent)
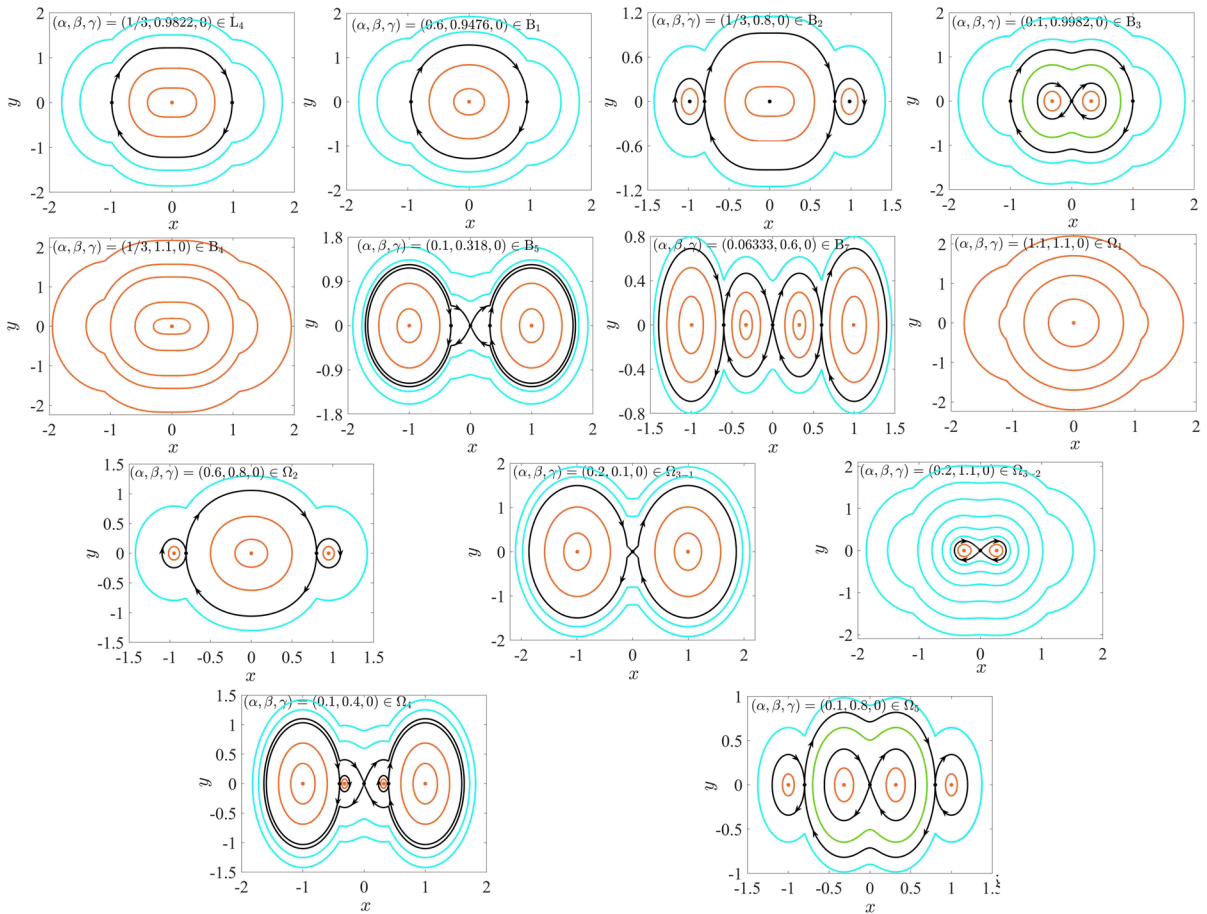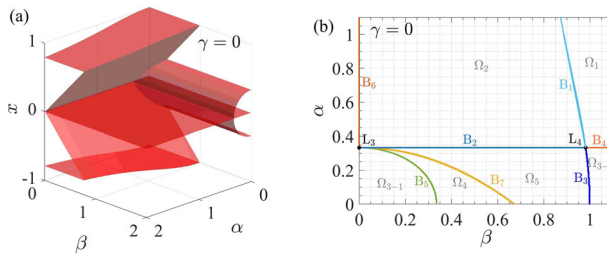
Fig. 15 Phase portraits for $\gamma = 0$ (The value of parameters and the belonged set are shown in each figure legend)

B Relationship between bifurcation surfaces and catastrophe curves

To prove the relationship between bifurcation surfaces and catastrophe curves shown in Eq. (8), set B_1 to B_7 are divided into a series of sets as shown in the following

$$\mathcal{M}_+ = \{(\alpha, \beta, \gamma) | \exists x_1 < 0 < x_2,$$

$$f(x_i) = f'(x_i) = 0, i = 1, 2, f''(x_1) < 0 < f''(x_2)\},$$
$$\mathcal{M}_- = \{(\alpha, \beta, \gamma) | \exists x_1 < 0 < x_2,$$
$$f(x_i) = f'(x_i) = 0, i = 1, 2, f''(x_1) > 0 > f''(x_2)\},$$
$$\mathcal{N}_- = \{(\alpha, \beta, \gamma) | \exists x > 0, f(x) < 0\},$$
$$\mathcal{N}_+ = \{(\alpha, \beta, \gamma) | \forall x > 0, f(x) > 0\},$$
$$\mathcal{E}_-^i = \{(\alpha, \beta, \gamma) | C_i(\alpha, \beta, \gamma) < 0\},$$
$$\mathcal{E}_+^i = \{(\alpha, \beta, \gamma) | C_i(\alpha, \beta, \gamma) > 0\}, \quad (i = 1, 3, 5)$$

$\mathcal{G} = \{(\alpha, \beta, \gamma) | \exists x_i,$

$V(x_i) = V(0), V'(x_i) = 0, V''(x_i) < 0, i = 1, 2\},$

$\mathcal{K} = \{(\alpha, \beta, \gamma) | \exists x_1 < 0 < x_2,$

$f(x_i) = f'(x_i) = f''(x) = 0, i = 1, 2\}.$

It is obvious that $\mathcal{N}_\pm$ and $\mathcal{E}_\pm^i$ are areas, $\mathcal{M}_\pm$ and $\mathcal{G}$ are surfaces, $\mathcal{K}$ is curve. And we have

$$\begin{cases} \mathcal{M}_+ \cap \mathcal{M}_- = \mathcal{N}_+ \cap \mathcal{N}_- = \mathcal{E}_+^i \cap \mathcal{E}_-^i = \varnothing, \quad \partial^2 \mathcal{E}_\pm^i = \varnothing \\ \partial \mathcal{E}_-^i = \partial \mathcal{E}_+^i = \{(\alpha, \beta, \gamma) | C_i(\alpha, \beta, \gamma) = 0\}, \\ \partial \mathcal{N}_- = \partial \mathcal{N}_+ = \mathcal{M}_+, \quad \partial \mathcal{M}_- = \partial \mathcal{M}_+ = \mathcal{K}. \end{cases}$$
(B1)

Also, we give some lemmas about the characteristics of restoring force $f(x)$ without proving:

Lemma 1 $f(-x) = -f(x), \lim_{x \to \pm\infty} f(x) = \pm\infty$ and $f^{(2n)}(0) = 0, n \in \mathbb{N}$;

Lemma 2 $f(x)$ has at most 3 zero points for $x \in (0, +\infty)$;

Lemma 3 $f(x)$ has at most 3 extreme points and 2 inflection points for $x \in (0, +\infty)$;

Lemma 4 if $f'(0) = f'''(0) = 0$, then $f^{(5)}(0) < 0 \iff (\alpha, \beta, \gamma) \in \mathcal{N}_-$;

Lemma 5 if $f'(0) = f'''(0) = 0$, then $f^{(5)}(0) > 0 \iff (\alpha, \beta, \gamma) \in \mathcal{N}_+$;

Lemma 6 if $f'(0) = 0$ and $(\alpha, \beta, \gamma) \in \mathcal{M}_+$, then $C_3(\alpha, \beta, \gamma) > 0$.
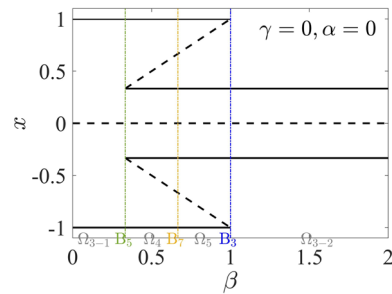
(1)

Set B_1 can be divided into $B_1 = \mathcal{E}_+^1 \cap \mathcal{M}_+$ and ∂B_1 can be divided into $\partial B_1 = (\partial \mathcal{E}_\pm^1 \cap \mathcal{M}_+) \cup (\mathcal{E}_+^1 \cap \partial \mathcal{M}_\pm) \cup (\partial \mathcal{E}_\pm^1 \cap \partial \mathcal{M}_\pm)$.

We have $\partial \mathcal{E}_\pm^1 \cap \mathcal{M}_+ = L_4$, $\partial \mathcal{E}_\pm^1 \cap \partial \mathcal{M}_\pm = P$ and

$$\mathcal{E}_+^1 \cap \partial \mathcal{M}_\pm = \lim_{x_i \to 0} \{(\alpha, \beta, \gamma) | C_1(\alpha, \beta, \gamma) > 0;$$

$$\exists x_1 < 0 < x_2, f(x_i) = f'(x_i) = 0, i = 1, 2, f''(x_1) < 0 < f''(x_2)\}.$$
(B2)

Assume that $f(x) = ax(x^2 - x_i^2)^2 + bx^3(x^2 - x_i^2)^3 + cx^5(x^2 - x_i^2)^4 + o(x^7)$, which is

$$f(x) = ax_i^4 x - (2ax_i^2 + bx_i^6)x^3 + (a + 3bx_i^4 + cx_i^8) x^5 + o(x^7),$$
(B3)

Fig. 16 Bifurcation diagrams for $\alpha = 0$ and $\gamma = 0$

and let Eq. (B3) be the Taylor series of the restoring force, so that $C_1(\alpha, \beta, \gamma) = ax_i^4$, $C_3(\alpha, \beta, \gamma) = -(2ax_i^2 + bx_i^6)$ and $C_5(\alpha, \beta, \gamma) = (a + 3bx_i^4 + cx_i^8)$, where $x_i = x_i(\alpha, \beta, \gamma)$ and $a > 0$. Let $x_i \to 0$ and we can obtain $\lim_{x_i \to 0} C_1(\alpha, \beta, \gamma) = 0$, $\lim_{x_i \to 0} C_3(\alpha, \beta, \gamma) = 0$ and $\lim_{x_i \to 0} C_5(\alpha, \beta, \gamma) = a > 0$.

Therefore, we have $\mathcal{E}_+^1 \cap \partial \mathcal{M}_\pm = L_5$, and $\partial B_1 = L_4 \cup L_5 \cup P$.
(2)

Set B_2 can be divided into $B_2 = \partial \mathcal{E}_\pm^1 \cap \mathcal{E}_+^3 \cap \mathcal{N}_-$ and ∂B_2 can be divided into $\partial B_2 = (\partial \mathcal{E}_\pm^1 \cap \partial \mathcal{E}_\pm^3 \cap \mathcal{N}_-) \cup (\partial \mathcal{E}_\pm^1 \cap \mathcal{E}_+^3 \cap \partial \mathcal{N}_\pm) \cup (\partial \mathcal{E}_\pm^1 \cap \partial \mathcal{E}_\pm^3 \cap \partial \mathcal{N}_\pm)$.

From lemma 4 we have $\partial \mathcal{E}_\pm^1 \cap \partial \mathcal{E}_\pm^3 \cap \mathcal{N}_- = L_3$, and form lemma 6 we have $\partial \mathcal{E}_\pm^1 \cap \mathcal{E}_+^3 \cap \partial \mathcal{N}_\pm = \partial \mathcal{E}_\pm^1 \cap \mathcal{M}_+ = \mathcal{L}_4$, we also have $\partial \mathcal{E}_\pm^1 \cap \partial \mathcal{E}_\pm^3 \cap \partial \mathcal{N}_\pm = P$. Therefore, $\partial B_2 = L_3 \cup L_4 \cup P$.
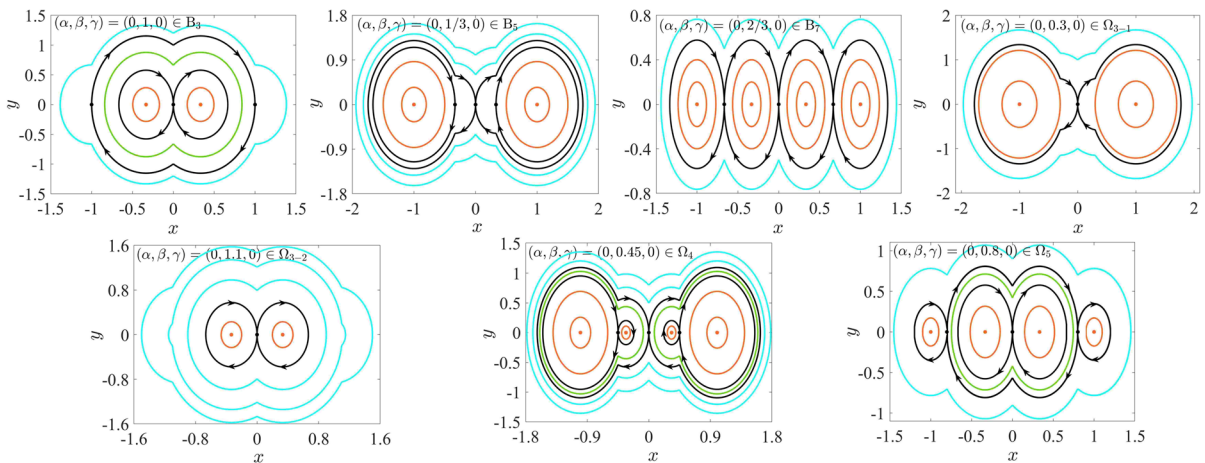(3)

Set B_3 can be divided into $B_3 = \mathcal{E}_-^1 \cap \mathcal{M}_+$ and ∂B_3 can be divided into $\partial B_3 = (\partial \mathcal{E}_\pm^1 \cap \mathcal{M}_+) \cup (\mathcal{E}_-^1 \cap \partial \mathcal{M}_\pm) \cup (\partial \mathcal{E}_\pm^1 \cap \partial \mathcal{M}_\pm)$.

It is obvious that $\partial \mathcal{E}_\pm^1 \cap \mathcal{M}_+ = L_4$, $\mathcal{E}_-^1 \cap \partial \mathcal{M}_\pm = \mathcal{E}_-^1 \cap \mathcal{K} = L_1$ and $\partial \mathcal{E}_\pm^1 \cap \partial \mathcal{M}_\pm = P$. Therefore, $\partial B_3 = L_1 \cup L_4 \cup P$.
(4)

Set B_4 can be divided into $B_4 = \partial \mathcal{E}_\pm^1 \cap \mathcal{E}_+^3 \cap \mathcal{N}_+$ and ∂B_4 can be divided into $\partial B_4 = (\partial \mathcal{E}_\pm^1 \cap \partial \mathcal{E}_\pm^3 \cap \mathcal{N}_+) \cup (\partial \mathcal{E}_\pm^1 \cap \mathcal{E}_+^3 \cap \partial \mathcal{N}_\pm) \cup (\partial \mathcal{E}_\pm^1 \cap \partial \mathcal{E}_\pm^3 \cap \partial \mathcal{N}_\pm)$.

From lemma 5 we have $\partial \mathcal{E}_\pm^1 \cap \partial \mathcal{E}_\pm^3 \cap \mathcal{N}_+ = L_5$. We also have $\partial \mathcal{E}_\pm^1 \cap \mathcal{E}_+^3 \cap \partial \mathcal{N}_\pm = L_4$ and $\partial \mathcal{E}_\pm^1 \cap \partial \mathcal{E}_\pm^3 \cap \partial \mathcal{N}_\pm = P$. Therefore, $\partial B_4 = L_4 \cup L_5 \cup P$.
(5)

Set B_5 can be divided into $B_5 = \mathcal{E}_-^1 \cap \mathcal{M}_-$ and ∂B_5 can be divided into $\partial B_5 = (\partial \mathcal{E}_\pm^1 \cap \mathcal{M}_-) \cup (\mathcal{E}_-^1 \cap \partial \mathcal{M}_\pm) \cup (\partial \mathcal{E}_\pm^1 \cap \partial \mathcal{M}_\pm)$.

Fig. 17 Phase portraits for $\alpha = 0$ and $\gamma = 0$ (The value of parameters and the belonged set are shown in each figure legend)

It is obvious that $\mathcal{E}_{\pm}^1 \cap \partial \mathcal{M}_{\pm} = L_1$, $\partial \mathcal{E}_{\pm}^1 \cap \partial \mathcal{M}_{\pm} = P$ and

$$\partial \mathcal{E}_{\pm}^1 \cap \mathcal{M}_- = \lim_{C_1 \to 0^-} \{(\alpha, \beta, \gamma) | C_1(\alpha, \beta, \gamma) < 0;$$
$$\exists x_1 < 0 < x_2,$$
$$f(x_i) = f'(x_i) = 0, i = 1, 2, f''(x_1) > 0 > f''(x_2)\}.$$
(B4)

Considering $f(0) = f(x_i) = 0$, $f'(0) < 0$, $f'(x_i) = 0$, $f''(0) = 0$, $f''(x_i) < 0$ and lemma 3, we have

(a). there exists minimum points $x_{\mathrm{I}} \in (0, x_i)$ and $\exists x_{\mathrm{II}} \in (x_i, +\infty)$, $f(x_{\mathrm{I}}) < 0$, $f(x_{\mathrm{II}}) < 0$, $f'(x_{\mathrm{I}}) = f'(x_{\mathrm{II}}) = 0$, $f''(x_{\mathrm{I}}) > 0$, $f''(x_{\mathrm{II}}) > 0$;
(b). $\exists x_a \in (x_{\mathrm{I}}, x_i)$, $\exists x_b \in (x_i, x_{\mathrm{II}})$, $f''(x_a) = 0$, $f''(x_b) = 0$;
(c). $f'(x)$ monotone increases in $(0, x_a)$, monotone decreases in (x_a, x_b) and monotone increases in $(x_b, +\infty)$.

So it is clear that

$$f(x_{\mathrm{I}}) = \int_0^{x_{\mathrm{I}}} f'(x) dx > f'(0) x_{\mathrm{I}},$$

let $f'(0) \to 0^-$ and we have $f(x_{\mathrm{I}}) \to 0^-$, then we have $f(x) \to 0^-$ for $\forall x \in (0, x_i)$ because $f(x_{\mathrm{I}}) \leq f(x) < 0$ in $(0, x_i)$. From lemma 2, it can be derived that

$$\lim_{f'(0) \to 0^-} x_i = 0.$$
(B5)

Assume that $f(x) = ax(x^2 - x_i^2)^2 + bx^3(x^2 - x_i^2)^3 + cx^5(x^2 - x_i^2)^4 + o(x^7)$ and $a < 0$, which is

the same form as Eq. (B3). Then let it be the Taylor series of the restoring force, so that $C_1(\alpha, \beta, \gamma) = a x_i^4$, $C_3(\alpha, \beta, \gamma) = -(2a x_i^2 + b x_i^6)$ and $C_5(\alpha, \beta, \gamma) = (a + 3b x_i^4 + c x_i^8)$, where $x_i = x_i(\alpha, \beta, \gamma)$ and $a > 0$. Let $x_i \to 0$ and we can obtain $\lim_{C_1 \to 0^-} C_3(\alpha, \beta, \gamma) = 0$ and $\lim_{C_1 \to 0^-} C_5(\alpha, \beta, \gamma) = a < 0$.

Therefore, we have $\partial \mathcal{E}_{\pm}^1 \cap \mathcal{M}_- = L_3$, and $\partial B_5 = L_1 \cup L_3 \cup P$.
(6)

Set B_6 can be divided into $B_6 = \partial \mathcal{E}_{\pm}^1 \cap \mathcal{E}_-^3$ and ∂B_6 can be divided into $\partial B_6 = \partial \mathcal{E}_{\pm}^1 \cap \mathcal{E}_{\pm}^3$, which is

$$\partial B_6 = \{(\alpha, \beta, \gamma) | C_1(\alpha, \beta, \gamma) = 0; C_3(\alpha, \beta, \gamma) = 0\}. \quad (B6)$$

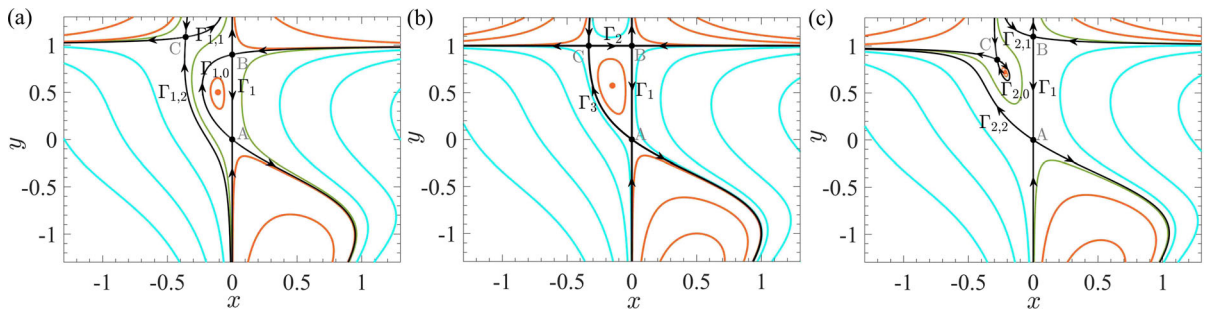It is obvious that $\partial B_6 = L_3 \cup L_5 \cup P$.
(7)

Set B_7 can be divided into $B_7 = \mathcal{E}_-^1 \cap \mathcal{G}$ and ∂B_7 can be divided into $\partial B_7 = (\partial \mathcal{E}_{\pm}^1 \cap \mathcal{G}) \cup (\mathcal{E}_-^1 \cap \partial \mathcal{G}) \cup (\partial \mathcal{E}_{\pm}^1 \cap \partial \mathcal{G})$, where

$$\partial \mathcal{G} = \{(\alpha, \beta, \gamma) | \exists x_1 < 0 < x_2, \quad (B6)$$
$$V(x_i) = V(0), V'(x_i) = V''(x_i) = 0, i = 1, 2\}.$$
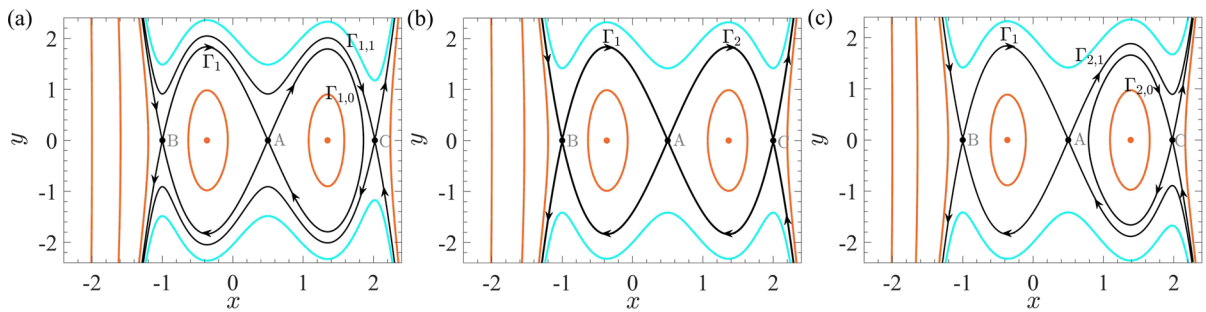
It is obvious that $\mathcal{E}_-^1 \cap \partial \mathcal{G} = L_2 \subseteq B_3$. And

$$\partial \mathcal{E}_{\pm}^1 \cap \mathcal{G} = \lim_{C_1 \to 0^-} \{(\alpha, \beta, \gamma) | C_1(\alpha, \beta, \gamma) < 0;$$
$$\exists x_1 < 0 < x_2,$$
$$V(x_i) = V(0), V'(x_i) = 0, V''(x_i) < 0, i = 1, 2\}.$$
(B7)

Fig. 18 Heteroclinic orbits for Hamilton system: **a** $a = 0.95, b = -1$; **b** $a = 1, b = -1$; **c** $a = 1.05, b = -1$

Fig. 19 Heteroclinic orbits for Hamilton system: **a** $a = \frac{1}{2}, b = -1, c = -4, q = 3.98$; **b** $a = \frac{1}{2}, b = -1, c = -4, q = 4$; **c** $a = \frac{1}{2}, b = -1, c = -4, q = 4.02$

Considering $\int_0^{x_i} f(x)dx = V(x_i) - V(0) = 0$, $f(x_i) = 0$, $f'(x_i) < 0$, lemma 1, lemma 2 and lemma 3, we have

(a). $\exists x_k \in (0, x_i)$, $x_j \in (x_i, +\infty)$, $f(x_k) = f(x_i) = f(x_j) = 0$;

(b). there exists minimum $x_I \in (0, x_k)$, maximum $x_{II} \in (x_k, x_i)$ and minimum $x_{III} \in (x_i, x_j)$, $f'(x_I) = f'(x_{II}) = f'(x_{III}) = 0$;

(c). $f'(x)$ monotone increases in $(0, x_I)$.

So it is clear that

$$f(x_I) = \int_0^{x_I} f'(x)dx > f'(0)x_I,$$

let $f'(0) \to 0^-$ and we have $f(x_I) \to 0^-$.

Considering $f(x_I)x_k < \int_0^{x_k} f(x)dx < 0$, we have $\int_0^{x_k} f(x)dx \to 0^-$ and $\int_{x_k}^{x_i} f(x)dx = -\int_0^{x_k} f(x)dx \to 0^+$. So it can be derived that $f(x) \to 0^-$ for $\forall x \in (0, x_k)$ and $f(x) \to 0^+$ for $\forall x \in (x_k, x_i)$.

From lemma 2, it can be derived that

$$\lim_{f'(0) \to 0^-} x_i = \lim_{f'(0) \to 0^-} x_k = 0. \tag{B8}$$

Assume that $V(x) = ax^2(x^2 - x_i^2)^2 + bx^4(x^2 - x_i^2)^3 + cx^6(x^2 - x_i^2)^4 + o(x^7)$, and $f(x) = V'(x)$,

which is

$$f(x) = 2ax_i^4 x - 4(2ax_i^2 + bx_i^6)x^3 + 6(a + 3bx_i^4 + cx_i^8)x^5 + o(x^7), \tag{B9}$$

and let Eq. (B9) be the Taylor series of the restoring force, so that $C_1(\alpha, \beta, \gamma) = 2ax_i^4$, $C_3(\alpha, \beta, \gamma) = -4(2ax_i^2 + bx_i^6)$ and $C_5(\alpha, \beta, \gamma) = 6(a + 3bx_i^4 + cx_i^8)$, where $x_i = x_i(\alpha, \beta, \gamma)$ and $a < 0$. Let $x_i \to 0$ and we can obtain $\lim_{C_1 \to 0} C_3(\alpha, \beta, \gamma) = 0$ and $\lim_{C_1 \to 0} C_5(\alpha, \beta, \gamma) = 6a < 0$.

Therefore, we have $\partial \mathcal{E}_\pm^1 \cap \mathcal{G} = L_3$, and $\partial B_7 = L_2 \cup L_3 \cup P$.

C Structural stability of Hamilton system with heteroclinic orbits

Without loss of generality, a 2-dimensional Hamilton system is considered, whose Hamilton function can be written in the following form

$$H(x, y) = \sum_{i=1}^{\infty} \sum_{j=1}^{\infty} a_{i,j} x^i y^j. \tag{C1}$$

two examples are given to illustrate the condition of heteroclinic bifurcation of 2-dimensional Hamilton system, which is shown in theorem 1.

Example 1 Let $a_{2,0} = 1, a_{1,1} = a, a_{1,2} = b, a_{2,3} = -1, a, b \in \mathbb{R}$ and $a_{i,j} \equiv 0$(else), the Hamilton function is $H(x, y, \boldsymbol{p}) = x^2 + axy + bxy^2 - x^2y^3$, where $\boldsymbol{p} = (a, b)^{\mathrm{T}}$, which leads to the following Hamilton system

$$\begin{cases} x' = ax + 2bxy - 3x^2y^2, \\ y' = -2x - ay - by^2 + 2xy^3. \end{cases} \quad (C2)$$

Three saddles A$(0, 0)$, B$(0, -\frac{a}{b})$ and $C(x_c(\boldsymbol{p}), y_c(\boldsymbol{p}))$ can be found. When $\boldsymbol{p} = (1, -1)^{\mathrm{T}}$, we have $H|_{\mathrm{A}} = H|_{\mathrm{B}} = H|_{\mathrm{C}} = 0$, thus three heteroclinic orbits can be found, as shown in Fig. 18b: Γ_1 connecting A$(0, 0)$ and B$(0, 1)$; Γ_2 connecting B$(0, 1)$ and C$(-\frac{1}{3}, 1)$; Γ_3 connecting A$(0, 0)$ and C$(-\frac{1}{3}, 1)$. Calculation shows that

$$\frac{\partial H}{\partial a}|_B - \frac{\partial H}{\partial a}|_A = 0,$$
$$\frac{\partial H}{\partial b}|_B - \frac{\partial H}{\partial b}|_A = 0,$$
$$\frac{\partial H}{\partial a}|_C - \frac{\partial H}{\partial a}|_B = x_c(\boldsymbol{p})y_c(\boldsymbol{p}) \neq 0,$$
$$\frac{\partial H}{\partial b}|_C - \frac{\partial H}{\partial b}|_B = x_c(\boldsymbol{p})y_c^2(\boldsymbol{p}) \neq 0,$$
$$\frac{\partial H}{\partial a}|_C - \frac{\partial H}{\partial a}|_A = x_c(\boldsymbol{p})y_c(\boldsymbol{p}) \neq 0,$$
$$\frac{\partial H}{\partial b}|_C - \frac{\partial H}{\partial b}|_A = x_c(\boldsymbol{p})y_c^2(\boldsymbol{p}) \neq 0,$$

which means heteroclinic orbit Γ_1 is structurally stable, but Γ_2 and Γ_3 are structurally unstable. The neighborhood systems are shown in Fig. 18a and c. Heteroclinic orbit Γ_2 splits into orbits $\Gamma_{1,0} \cup \Gamma_{1,1}$ or $\Gamma_{2,0} \cup \Gamma_{2,1}$, while heteroclinic orbit Γ_3 splits into orbits $\Gamma_{1,0} \cup \Gamma_{1,2}$ or $\Gamma_{2,0} \cup \Gamma_{2,2}$.

Example 2 Consider the Hamilton function $H(x, y, \boldsymbol{p}) = \frac{1}{2}y^2 - (x - a)^2(x - b)^2(x^2 + cx + q)$, where $\boldsymbol{p} = (a, b, c, q)^{\mathrm{T}}$, which leads to the following Hamilton system

$$\begin{cases} x' = y, \\ y' = 2(x - a)(x - b)(2x - a - b)(x^2 + cx + q) \\ \quad + (x - a)^2(x - b)^2(2x + c). \end{cases}$$
$$(C3)$$

Three saddles A$(a, 0)$, B$(b, 0)$ and $C(x_c(\boldsymbol{p}), 0)$ can be found. When $\boldsymbol{p} = (\frac{1}{2}, -1, -4, 4)^{\mathrm{T}}$, we have $H|_{\mathrm{A}} = H|_{\mathrm{B}} = H|_{\mathrm{C}} = 0$, and two heteroclinic orbits can be found, as shown in Fig. 19b: Γ_1 connecting A$(\frac{1}{2}, 0)$ and B$(-1, 0)$; Γ_2 connecting A$(\frac{1}{2}, 0)$ and C$(x_c(\boldsymbol{p}), 0)$. Calculation shows that

$$\frac{\partial H}{\partial p_i}|_A - \frac{\partial H}{\partial p_i}|_B = 0 \ (p_i = a, b, c, q),$$
$$\frac{\partial H}{\partial c}|_C - \frac{\partial H}{\partial c}|_A = -x_c(\boldsymbol{p})(x_c(\boldsymbol{p}) - a)^2(x_c(\boldsymbol{p}) - b)^2 \neq 0,$$
$$\frac{\partial H}{\partial q}|_C - \frac{\partial H}{\partial q}|_A = -(x_c(\boldsymbol{p}) - a)^2(x_c(\boldsymbol{p}) - b)^2 \neq 0,$$

which means heteroclinic orbit Γ_1 is structurally stable, but Γ_2 is structurally unstable. The neighborhood systems are shown in Fig. 19a and c. Heteroclinic orbit Γ_2 splits into orbits $\Gamma_{1,0} \cup \Gamma_{1,1}$ or $\Gamma_{2,0} \cup \Gamma_{2,1}$.

References

1. Hayashi, C.: Nonlinear Oscillations in Physical Systems. Princeton University Press, Princeton (2014)
2. Lenci, S., Rega, G.: Regular nonlinear dynamics and bifurcations of an impacting system under general periodic excitation. Nonlinear Dyn. **34**, 249–268 (2003)
3. Várkonyi, P., Domokos, G.: Symmetry, optima and bifurcations in structural design. Nonlinear Dyn. **43**, 47–58 (2006)
4. Padthe, A., Chaturvedi, N., Bernstein, D., et al.: Feedback stabilization of snap-through buckling in a preloaded two-bar linkage with hysteresis. Int. J. Non Linear Mech. **43**(4), 277–291 (2008)
5. Avramov, K., Mikhlin, Y.: Snap-through truss as a vibration absorber. J. Vib. Control **10**(2), 291–308 (2004)
6. Carrella, A., Brennan, M., Waters, T.: Static analysis of a passive vibration isolator with quasi-zero-stiffness characteristic. J. Sound Vib. **301**, 678–689 (2007)
7. Kovacic, I., Brennan, M., Waters, T.: A study of a nonlinear vibration isolator with a quasi-zero stiffness characteristic. J. Sound Vib. **315**(3), 700–711 (2008)
8. Carrella, A., Brennan, M.J., Kovacic, I., et al.: On the force transmissibility of a vibration isolator with quasi-zero-stiffness. J. Sound Vib. **332**, 707–717 (2009)
9. Carrella, A., Friswell, M., Zotov, A., et al.: Using nonlinear springs to reduce the whirling of a rotating shaft. Mech. Syst. Signal Process. **23**, 2228–2235 (2009)
10. Zhu, G., Liu, J., Cao, Q., et al.: A two degree of freedom stable quasi-zero stiffness prototype and its applications in aseismic engineering. Sci. China Technol. Sci. **63**(3), 496–505 (2020)
11. Thomson, A., Thompson, W.: Dynamics of a bistable system: the "click" mechanism in dipteran flight. Acta Biotheor **26**(1), 19–29 (1977)

12. Brennan, M., Elliott, S., Bonello, P., et al.: The "click" mechanism in dipteran flight: if it exists, then what effect does it have? J. Theor. Biol **224**(2), 205–213 (2003)
13. Lenz, M., Crow, D., Joanny, J.: Membrane buckling induced by curved filaments. Phys. Rev. lett. **103**(3), 038101 (2009)
14. Dawson, J.: Nonlinear electron oscillations in a cold plasma. Phys. Rev. **113**(2), 383 (1959)
15. Tonks, L.: Oscillations in ionized gases. Plasma and Oscillations. Pergamon, PP. 122–139 (1961)
16. Calvayrac, F., Reinhard, P., Suraud, E., et al.: Nonlinear electron dynamics in metal clusters. Phys. Rep. **337**(6), 493–578 (2000)
17. Duffing, G.: Erzwungene schwingungen bei veränderlicher eigenfrequenz[J], p. 7. Braunschweig, Vieweg u. Sohn (1918)
18. Carrella, A., Friswell, M., Zotov, A., et al.: Using nonlinear springs to reduce the whirling of a rotating shaft. Mech. Syst. Signal Process. **23**, 2228–2235 (2009)
19. Carrella, A., Brennan, M., Waters, T., et al.: Force and displacement transmissibility of a nonlinear isolator with high-static-low-dynamic stiffness. Int. J. Mech. Sci. **55**(1), 22–29 (2012)
20. Kanamaru, T.: Van der Pol oscillator. Scholarpedia **2**(1), 2202 (2007)
21. Pleijel, Å.: Some remarks about the limit point and limit circle theory. Arkiv för Matematik **7**(6), 543–550 (1969)
22. Ueda, Y.: Randomly transitional phenomena in the system governed by Duffing's equation. J. Stat. Phys. **20**, 181–196 (1979)
23. Edward, N.: Deterministic nonperiodic flow. J. Atmos. Sci. **20**(2), 130–141 (1963)
24. Cao, Q., Wiercigroch, M., Pavlovskaia, E., et al.: Archetypal oscillator for smooth and discontinuous dynamics. Phys. Rev. E **74**(4), 046218 (2006)
25. Tian, R., Cao, Q., Li, Z.: Hopf bifurcations for the recently proposed smooth-and-discontinuous oscillator. Chinese Phys. Lett. **27**(7), 074701 (2010)
26. Tian, R., Cao, Q., Yang, S.: The codimension-two bifurcation for the recent proposed SD oscillator. Nonlinear Dyn. **59**(1–2), 19 (2010)
27. Tian, R., Yang, X., Cao, Q., et al.: Bifurcations and chaotic threshold for a nonlinear system with an irrational restoring force. Chinese Phys. B **21**(2), 020503 (2012)
28. Cao, Q., Xiong, Y., Wiercigroch, M.: Resonances of the SD oscillator due to the discontinuous phase. J. Appl. Anal. Comput. **1**(2), 183–191 (2011)
29. Zhang, Y., Cao, Q.: The recent advances for an archetypal smooth and discontinuous oscillator. Int. J. Mech. Sci. **214**, 106904 (2022)
30. Han, Y., Cao, Q., Chen, Y., et al.: A novel smooth and discontinuous oscillator with strong irrational nonlinearities. Sci. China Phys. Mech. Astron. **55**, 1832–1843 (2012)
31. Han, Y., Cao, Q., Chen, Y., et al.: A novel smooth and discontinuous oscillator with strong irrational nonlinearities. Sci. China Phys. Mech. Astron. **55**, 1832–1843 (2012)
32. Cao, Q., Han, Y., Liang, T., et al.: Multiple buckling and codimension-three bifurcation phenomena of a nonlinear oscillator. Int. J. Bifurcation Chaos **24**(01), 1430005 (2014)
33. Han, Y., Cao, Q., Ji, J.: Nonlinear dynamics of a smooth and discontinuous oscillator with multiple stability. Int. J. Bifur. Chaos **25**(13), 1530038 (2015)
34. Zhu, G., Cao, Q., Wang, Z., et al.: Road to entire insulation for resonances from a forced mechanical system. Sci. Rep. **12**(1), 21167 (2022)
35. Han, Y.: Nonlinear dynamics of a class of geometrical nonlinear system and its application. PhD thesis. Harbin Institute of Technology (2015)
36. Dangelmayr, G., Wegelin, M.: On a codimension-four bifurcation occurring in optical bistability. Singularity Theory and its Applications: Warwick, Part II: Singularities, Bifurcations and Dynamics. Springer, Berlin, **2006**, 107–121 (1989)
37. Krauskopf, B., Osinga, H.: A codimension-four singularity with potential for action. Mathematical Sciences with Multidisciplinary Applications: In Honor of Professor Christiane Rousseau. And In Recognition of the Mathematics for Planet Earth Initiative. Springer International Publishing, PP. 253–268 (2016)
38. Eilertsen, J., Magnan, J.: On the chaotic dynamics associated with the center manifold equations of double-diffusive convection near a codimension-four bifurcation point at moderate thermal Rayleigh number[J]. Int. J. Bifur. Chaos **28**(08), 1850094 (2018)
39. Guckenheimer, J., Holmes, P.: Structurally stable heteroclinic cycles. In: Mathematical Proceedings of the Cambridge Philosophical Society. Cambridge University Press, **103**(1), 189–192 (1988)
40. Armbruster, D., Chossat, P., Oprea, I.: Structurally stable heteroclinic cycles and the dynamo dynamics. Dynamo and Dynamics, a Mathematical Challenge, PP. 313–322 (2001)
41. Rabinowitz, P.: Heteroclinics for a Hamiltonian system of double pendulum type. J Juliusz Schauder Center **9**, 41–76 (1997)
42. Wang, L., Benenti, G., Casati, G., et al.: Ratchet effect and the transporting islands in the chaotic sea. Phys. Rev. Lett. **99**(24), 244101 (2007)
43. Lichtenberg, A., Lieberman, M.: Regular and Chaotic Dynamics. Springer, New York (1992)
44. Sagdeev, R., Usikov, D., Zakharov, M., et al.: Minimal chaos and stochastic webs. Nature **326**(6113), 559–563 (1987)
45. Daza, A., Wagemakers, A., Sanjuán, M., et al.: Testing for Basins of Wada. Sci. Rep. **5**, 16579 (2015). https://doi.org/10.1038/srep16579
46. Zhang, Y.: Wada basin boundaries and generalized basin cells in a smooth and discontinuous oscillator. Nonlinear Dyn. **106**, 2879–2891 (2021). https://doi.org/10.1007/s11071-021-06926-x